Predicting effective properties of Multiferroic composites

Thesis submitted to the

Indian Institute of Technology Bhubaneswar

For award of the Degree

of

Bachelor of Technology

By

Chaitanya Shah
15MM01007

Under the guidance of

Dr. Kaushik Das

IIT Bhubaneswar

School of Minerals, Metallurgical and Materials Engineering

Indian Institute of Technology Bhubaneswar

26th April 2019

Approval of the viva-voce board

26th April 2019

Certified that the thesis entitled “Predicting effective properties of Multiferroic composites”, submitted by Mr. Chaitanya Shah to Indian Institute of Technology, Bhubaneswar for the award of the degree Bachelor of technology has been accepted by the external examiners and the student has successfully defended the thesis in the viva-voce examination held today.

(Supervisor) (HOS) (External Examiner)

Certificate

This is to certify that the thesis entitled “Predicting effective properties of Multiferroic composites” submitted by Mr. Chaitanya Shah(15MM01007) to Indian Institute of Technology Bhubaneswar is a record of bonafide research work under my supervision and I consider it worthy of consideration for the award of the degree of Bachelor of Technology of the Institute

Dr. Kaushik Das
School of Minerals, Metallurgical and Materials Engineering
Indian Institute of Technology Bhubaneswar

26th April 2019

Declaration

I hereby declare that:

a. The work contained in this thesis is original and has been done by me under the guidance of my supervisor(s).

b. The work has not been submitted to any other institute for any degree or diploma.

c. I have followed the guidelines provided by the institute in writing the thesis

d. I have conformed to the norms and guidelines given in the Ethical code of conduct of the Institute.

e. Whenever I have used materials (data, theoretical analysis figures, text) from other sources, I have given due credit to them by citing them in the text of the thesis and giving their details in the references.

Signature of the student

Acknowledgments

First of all, I would like to express my sincere gratitude towards my supervisor, Dr. Kaushik Das for the constant support, motivation and guidance provided all throughout the year. Without his guidance and constant motivation, I would not have been able to start off and complete this project successfully. It was a great learning experience working under him. I will always cherish the academic and personal interaction I have had with him.

I would also like to thank Ms. Neelam Misra, PHD Scholar IIT Bhubaneswar who helped me getting familiarized with COMSOL and the basic theory of piezoelectric properties.

Last but not the least, I would dedicate this success to my parents and family members who constantly stood behind me and motivated me to give my best. This dissertation would not have been possible without the love and support of my family and friends.

Abstract

A multiferroic composite is a 2-phase composite where both the phases are ferroic phases. The definition of ferroic phases is that it has 2 or more orientation states in the absence of magnetic field, electric field, and mechanical stress; and it can shift from one state to another by means of a magnetic field, an electric field, a mechanical stress, or a combination of all.

In this research we will be considering a multiferroic composite consisting of piezoelectric (or piezomagnetic) as phase and piezomagnetic(or piezoelectric) as inclusion for different volume fractions and different aspect ratios(0,1,∞). The interface between the matrix and the inclusion can be perfect as well as imperfect, therefore we'll consider both the models in the research.

Among the many elastic, piezoelectric, piezomagnetic properties we will also be calculating Magnetoelectric coupling coefficients (α_{33} and α_{11}) which are absent in both piezoelectric and piezomagnetic materials. This is what is called the " 0+0->1 " product because neither of the piezoelectric and piezomagnetic phases exhibit magnetoelectric effect by itself but when combined, their composite exhibits magnetoelectric effect.

The advantage of multiferroic composites exhibiting magneto electric coupling is, the Electric-field control of magnetism. The production of electric fields is far less energy intensive than production of magnetic fields and this application could be technologically transformative.

It is important for us to predict the effective properties of Multiferroic composites so that we can figure out if it is feasible to synthesize the composite.

We'll start the research by analyzing the Elastic and Piezoelectric properties of a composite using Finite Element Analysis in COMSOL. Then we'll use micromechanical approach to find the effective properties of magnetoelectric composites using Mori-Tanaka method in MATLAB. We'll be using barium titanate ($BaTiO_3$ or BTO) as matrix (or inclusion) and cobalt ferrite($CoFe_2O_4$ or CFO) as inclusion (or matrix).

Table of Contents

List of Figures

Chapter 1 Introduction

1.1 Background

Multiferroic composites are 2-phase composite where both the phases are ferroic phases. Here the definition of a ferroic crystal is as follows:

(a) it has two or more orientation states in the absence of magnetic field, electric field, and mechanical stress; and

(b) it can shift from one state to another by means of a magnetic field, an electric field, a mechanical stress, or a combination of these[1]. Many combination of multiferroic composites with piezoelectric and piezomagnetic materials are possible. Piezoelectric materials that can be used include barium titanate ($BaTiO_3$ or BTO), lead zirconium titanate (PZT), and lead magnesium titanate - lead titanate (PMT-PT) and piezomagnetic materials that can be used include cobalt ferrite ($CoFe_2O_4$ or CFO), Terfenol-D, lanthanum strontium manganite (LSMO), and nickel ferrite (NFO). Strong coupling between the elastic, piezoelectric, dielectric, piezomagnetic, and magnetic properties of the constituent phases in a multiferroic composite with piezoelectric (or piezomagnetic) as phase and piezomagnetic (or piezoelectric) as inclusion make them the interesting of all the possible combinations of piezoelectric and piezomagnetic. In these types of composites, both the piezoelectric as well as the piezomagnetic phase are transversely isotropic. The most intriguing property of these composites is to exhibit magnetization under an electric field and polarization under a magnetic field. This property is called magnetoelectric effect, in other words these composites have non-zero magnetoelectric coupling coefficients (α_{33} and α_{11}). Here α_{ii} represents the induced axial magnetization, B_i, under an unit axial electric field, E_i, or conversely, the induced axial electric displacement, D_i, under an unit axial magnetic field, H_i, of the composite. This is what is called the " 0+0->1 " product because neither of the piezoelectric and piezomagnetic phases exhibit magnetoelectric effect by itself but when combined, their composite exhibits magnetoelectric effect.

In this project we'll consider a 2-phase composite consisting of piezoelectric (or piezomagnetic) phase and piezomagnetic (or piezoelectric) inclusion. Piezoelectric and piezomagnetic material that we'll be using are barium titanate ($BaTiO_3$ or BTO) and

cobalt ferrite ($CoFe_2O_4$ or CFO) respectively. Both the matrix and inclusion phase are transversely isotropic, with direction 3 representing the symmetric axis and plane 1-2 isotopic. Therefore we have overall 17 independent material constants which includes 5 elastic constants, C_{11}, C_{12}, C_{13}, C_{33}, C_{44}; 2 dielectric constants, κ_{11}, κ_{33}; 2 magnetic constants, μ_{11}, μ_{33}; piezoelectric constants, e_{15}, e_{31}, e_{33}; 3 piezomagnetic constants, q_{15}, q_{31}, q_{33} and 2 magnetoelectric constants, α_{33}, α_{11}.

We derive an important from the above mentioned coefficients, the magnetoelectric effect voltage coefficient α_{E33}. It is calculated by dividing the magnetoelectric coefficient, α_{33} and electric permittivity coefficient κ_{33}.

The aspect ratios (length to diameter ratio) that I'll be using are 0,1,∞. These 3 types are shown in Fig. 2. a-c and they are commonly referred as 2-2, 0-3, 1-3 connectivities. Along with the different ratios, even the interface between phase and inclusion can be perfect and imperfect. In an imperfect interface we assume that there is a thin layer on the surface of the inclusion which can be piezoelectric or piezomagnetic and collectively the inclusion and thin layer form a thinly coated inclusion.

1.2 Applications

Even before the multiferroic composites, the magnetoelectric effect was first observed in antiferromagnetic Cr_2O_3 at room temperature with magnetoelectric effect voltage coefficient of the order of 20 mV/cmOe. The multiferroic composites formed from piezomagnetic and piezoelectric phases have magnetoelectric effect voltage coefficient value greater than Cr_2O_3 and also greater than some other single-phase magnetoelectric material which finds them applications in various areas.

One of the major applications of Multiferroic composites, specifically Magnetoelectric composites is the Electric-field control of magnetism. The production of electric fields is far less energy intensive than production of magnetic fields and therefore, this application can transform the current scenario of technology. Until now, only a few successes have been reported in controlling the orientation of magnetism using an electric field, for example in heterostructures of conventional ferromagnetic metals and

multiferroic $BiFeO_3$ as well as in controlling the magnetic state, for example from antiferromagnetic to ferromagnetic in FeRh.

When a magnetic field is applied on a magnetoelectric composite, the magnetic phase in the composite strains, which produces a proportional charge in the piezoelectric phase. This property makes them suitable for making magnetic sensors. Sensitivity of the sensor can be increased by choosing a composite that has high magnetoelectric coefficient value.

Another important application of Magnetoelectric composite could be in memory devices where data can be written electronically and read magnetically.

Multiferroics have also been used to address the fundamental questions in particle physics and cosmology owing to the fact that an electron is an ideal multiferroic.

Multiferroics have also found applications that are not related to their magnetoelectric property, mostly in multiferroic bismuth ferrite. These applications include a photovoltaic effect, photocatalysis and gas sensing behaviour.

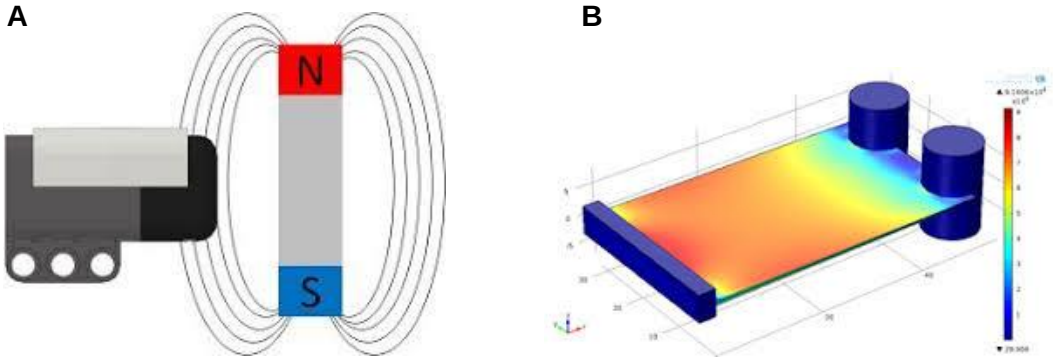

Fig 1.Applications (a) Magnetic Sensor (b) Vibration based energy harvestor

Chapter 2 Literature Review

The main feature of multiferroic materials which finds them various applications is the existence of a coupling between magnetism and polarization, i.e. magnetoelectricity. The origin of magnetoelectric effect can be different in different available multiferroic systems but the underlying effect is the same.

Till 1960's the researchers did not have any relations between the elastic properties of the constituent phases and the composite. It wasn't until 1964 when Hill[2] gave the first theory that the overall elastic moduli of fibre composites having transversely isotropic phases are connected by simple universal relations which are independent of the geometry at a given concentration. Then in 1989 Milgrom and Shtrikman[3] considered that were made of two isotropic materials and theorised that the moduli of the composite must obey a number of compatibility relations, involving the moduli of the components, but totally independent of the mixture ratio of the components and the microstructure of the composite.

The " 0+0->1 " product effect was first reported by van Suchtelen[4] in 1972 but it wasn't theoretically explained at that time. Then in 1994, the theoretical reason behind this principle was explained by the Green's function formulation put forward by Nan[5]. Nan was also the one of the first ones to think that the magnetic coupling coefficients (α_{33} and α_{11}) could depend on the size and shape of inclusion and hence, he computed the aspect ratio dependence of the magneto coupling coefficients by using the properties of BTO and CFO. Then later in 1995, Benveniste[6] also presented a theory to determine the magnetic coupling coefficients (α_{33} and α_{11}) of a fibrous piezoelectric-piezomagnetic composite using the results theorized by Hill (1964) and Milgrom and Shtrikman (1989). If is often said that the compatibility of the elastic strains of the piezoelectric and piezomagnetic phase determine the magnetic coupling coefficients (α_{33} and α_{11}) of the composite but the explicit expressions of magnetic coupling coefficient, α_{33}, of the fibrous composite given by Nan(1994) and Benveniste(1995) proved otherwise. The expression vividly showed that the elastic, piezoelectric and piezomagnetic constants of the constituent phases jointly contribute to the magnetic coupling coefficient.

After the Nan's Green's function approach to evaluate the Eshelby's[7] S-tensor, many of the researchers started to analyze the Green's function in a transversely isotropic piezoelectric (or piezomagnetic) medium as well as for the fibrous and lamellar and spherical inclusion.

Research	Author
Analyze Green's function of 3-D piezoelectric material	Wang[8] (1992), Chen[9],[10] (1993a,b,1997), Dunn and Taya[11] (1993a), Dunn and Wienecke[12] (1996)
Explicit components of S-tensor for fibrous and lamellar inclusion	Dunn and Taya[13] (1993b), Dunn (1994), Huang and Yu[14] (1994), Huang[15] (1997), Li and Dunn[16] (1998a), Mikita[17],[18] (2000,2001)
Explicit components of S-tensor for spheroidal inclusion	Huang and Kuo[15] (1997), Li and Dunn (1998b), Srinivas et al.[19] (2006)

All these works were concerned with the perfect interface case. One of the first studies to consider an imperfect interface was by Wang and Pan[20] for the case of fibrous composite. After that many studies have been conducted by various researchers to calculate the overall properties of the imperfectly bonded fibrous composite but the works have been limited to to study the imperfect interface for fibrous composites only.

Chapter 3 Predicting Effective properties of Multiferroic composites

Multiferroic composites are 2-phase composite where both the phases are ferroic phases and multiferroic as a whole exhibit more than one of the primary ferroic properties:

- Ferromagnetism: A magnetisation which can be switched by an application of magnetic field,
- Ferroelectricity: An electric polarisation which can be switched by an application of electric field, and
- Ferroelasticity: A deformation which can be switched by an application of stress.

The piezoelectric or piezomagnetic phase in a multiferroic composite will exhibit its usual electroelastic or magnetoelastic coupling .The piezoelectric nor the piezomagnetic phase exhibit magnetoelectric coupling but when they are combined in multiferroic composite, then the composite exhibits magnetoelectric coupling. Therefore to understand magnetoelectric coupling in a multiferroic composite it is important for us to understand the elastic, piezoelectric and piezomagnetic properties of a material.

3.1 Elastic Properties

Elastic Properties of a composite of are dependent of the material of matrix, reinforcement as well the volume fraction and aspect ratio of the reinforcement. Apart from this the elastic properties are also dependent on the material symmetry of the matrix and the reinforcement. We can control the volume fraction and aspect ratio but rest of the properties are dependent on the material. A material is anisotropic if its properties are direction dependent, isotropic when properties are same in all directions and transversely isotropic when properties are same in one plane and different in direction perpendicular to the plane. An anisotropic material has 27 independent constants, isotropic has 2 and transversely isotropic has 5 independent constants. We can find out the effective elastic properties in a composite using Hooke’s law by fixing

the strain value (displacement) and calculating the stresses developed in the material using COMSOL.

$$\sigma_{ij} = C_{ijkl}\varepsilon_{kl}$$

The generalized Hooke's law for a material is given as

where i,j,k,l=1,2,3

Here, σ_{ij} is a 2nd order tensor known as the stress tensor and its individual elements are the stress components, ε_{ij} is another 2nd order tensor known as the strain tensor and its individual elements are the strain components and C_{ijkl} is a 4th order tensor known as the stiffness tensor.

$$\begin{bmatrix} \sigma_1 = \sigma_{xx} \\ \sigma_2 = \sigma_{yy} \\ \sigma_3 = \sigma_{zz} \\ \sigma_4 = \sigma_{yz} \\ \sigma_5 = \sigma_{xz} \\ \sigma_6 = \sigma_{xy} \end{bmatrix} = \begin{bmatrix} C_{11} & C_{12} & C_{13} & C_{14} & C_{15} & C_{16} \\ C_{21} & C_{22} & C_{23} & C_{24} & C_{25} & C_{26} \\ C_{31} & C_{32} & C_{33} & C_{34} & C_{35} & C_{36} \\ C_{41} & C_{42} & C_{43} & C_{44} & C_{45} & C_{46} \\ C_{51} & C_{52} & C_{53} & C_{54} & C_{55} & C_{56} \\ C_{61} & C_{62} & C_{63} & C_{64} & C_{65} & C_{66} \end{bmatrix} \begin{bmatrix} \varepsilon_1 = \varepsilon_{xx} \\ \varepsilon_2 = \varepsilon_{yy} \\ \varepsilon_3 = \varepsilon_{zz} \\ \varepsilon_4 = \varepsilon_{yz} \\ \varepsilon_5 = \varepsilon_{xz} \\ \varepsilon_6 = \varepsilon_{xy} \end{bmatrix} \quad \text{(A)}$$

Matrix Representation of Hooke's law

The constitutive equation for elastic materials is,

$$\varepsilon = S\sigma \quad \text{(1)}$$

By inverting the above matrix formula so that strains are given explicitly in terms of stresses we get,

$$\begin{bmatrix}\varepsilon_1\\ \varepsilon_2\\ \varepsilon_3\\ \varepsilon_4\\ \varepsilon_5\\ \varepsilon_6\end{bmatrix}=\begin{bmatrix}S_{11} & S_{12} & S_{13} & S_{14} & S_{15} & S_{16}\\ S_{21} & S_{22} & S_{23} & S_{24} & S_{25} & S_{26}\\ S_{31} & S_{32} & S_{33} & S_{34} & S_{35} & S_{36}\\ S_{41} & S_{42} & S_{43} & S_{44} & S_{45} & S_{46}\\ S_{51} & S_{52} & S_{53} & S_{54} & S_{55} & S_{56}\\ S_{61} & S_{62} & S_{63} & S_{64} & S_{65} & S_{66}\end{bmatrix}\begin{bmatrix}\sigma_1\\ \sigma_2\\ \sigma_3\\ \sigma_4\\ \sigma_5\\ \sigma_6\end{bmatrix} \quad \text{(B)}$$

Matrix Representation of Constitutive equation

Depending on the symmetricity of the material, the matrix is reduced to a simpler form. Consider a transversely isotropic material symmetric about the z-axis. This makes x-y, the plane of isotropy. Consider an element of transversely isotropic material subjected to normal strain $\varepsilon_1(\varepsilon_{xx})$ of magnitude of ε, and also a normal strain of $\varepsilon_2(\varepsilon_{yy})$ of the same magnitude of ε.

Stresses induced by strain $\varepsilon_1 = \varepsilon$ only are

$$\sigma_1 = C_{11}\varepsilon;\ \sigma_2 = C_{21}\varepsilon;\ \sigma_3 = C_{31}\varepsilon;\ \sigma_4 = 0;\ \sigma_5 = 0;\ \sigma_6 = 0$$

Stresses induced by strain $\varepsilon_2 = \varepsilon$ only are

$$\sigma_1' = C_{11}\varepsilon;\ \sigma_2' = C_{21}\varepsilon;\ \sigma_3' = C_{31}\varepsilon;\ \sigma_4' = 0;\ \sigma_5' = 0;\ \sigma_6' = 0$$

Because of isotropy, the σ_1 (σ_{xx}) due to the ε_1 should be the same as the σ_2 (σ_{yy}) due to the ε_1. Therefore $C_{11}=C_{22}$. Further σ_3 (σ_{zz}) should be same for both, and so $C_{31}=C_{32}$. From further deformations we find that $C_{44}=C_{55}$ and $C_{66}=C_{11}-C_{12}$.

The stiffness matrix is thus reduced, and there are only 5 independent constants.

$$\begin{bmatrix}\sigma_1\\ \sigma_2\\ \sigma_3\\ \sigma_4\\ \sigma_5\\ \sigma_6\end{bmatrix}=\begin{bmatrix}C_{11} & C_{12} & C_{13} & 0 & 0 & 0\\ & C_{11} & C_{13} & 0 & 0 & 0\\ & & C_{33} & 0 & 0 & 0\\ & & & C_{44} & 0 & 0\\ & & & & C_{44} & 0\\ & & & & & C_{11}-C_{12}\end{bmatrix}\begin{bmatrix}\varepsilon_1\\ \varepsilon_2\\ \varepsilon_3\\ \varepsilon_4\\ \varepsilon_5\\ \varepsilon_6\end{bmatrix} \quad \text{(C)}$$

Matrix Representation of Hooke's law for transversely isotropic material

Rest of the part of the stiffness matrix is not written because the stiffness matrix is symmetric.

By inverting the above matrix formula so that strains are given explicitly in terms of stresses, we get the compliance matrix from which we can find the elastic constants E,v and G.

$$E_1 = E_2; \nu_{12} = \nu_{21}; \nu_{13} = \nu_{23}; \nu_{31} = \nu_{32}; G_{13} = G_{23}$$

$$\begin{bmatrix} \varepsilon_1 \\ \varepsilon_2 \\ \varepsilon_3 \\ \varepsilon_4 \\ \varepsilon_5 \\ \varepsilon_6 \end{bmatrix} = \begin{bmatrix} \frac{1}{E_1} & -\frac{\nu_{12}}{E_1} & -\frac{\nu_{31}}{E_3} & 0 & 0 & 0 \\ -\frac{\nu_{12}}{E_1} & \frac{1}{E_1} & -\frac{\nu_{31}}{E_3} & 0 & 0 & 0 \\ -\frac{\nu_{13}}{E_1} & -\frac{\nu_{13}}{E_1} & \frac{1}{E_3} & 0 & 0 & 0 \\ 0 & 0 & 0 & \frac{1}{2G_{13}} & 0 & 0 \\ 0 & 0 & 0 & 0 & \frac{1}{2G_{13}} & 0 \\ 0 & 0 & 0 & 0 & 0 & \frac{1}{2G_{12}} \end{bmatrix} \begin{bmatrix} \sigma_1 \\ \sigma_2 \\ \sigma_3 \\ \sigma_4 \\ \sigma_5 \\ \sigma_6 \end{bmatrix} \quad \text{(D)}$$

Matrix Representation of Constitutive equation in terms on elastic constants

Same way for an isotropic material the stiffness matrix is reduced to only 2 independent constants.

$$\begin{bmatrix} \sigma_1 \\ \sigma_2 \\ \sigma_3 \\ \sigma_4 \\ \sigma_5 \\ \sigma_6 \end{bmatrix} = \begin{bmatrix} C_{11} & C_{12} & C_{12} & 0 & 0 & 0 \\ & C_{11} & C_{12} & 0 & 0 & 0 \\ & & C_{11} & 0 & 0 & 0 \\ & & & C_{11}-C_{12} & 0 & 0 \\ & & & & C_{11}-C_{12} & 0 \\ & & & & & C_{11}-C_{12} \end{bmatrix} \begin{bmatrix} \varepsilon_1 \\ \varepsilon_2 \\ \varepsilon_3 \\ \varepsilon_4 \\ \varepsilon_5 \\ \varepsilon_6 \end{bmatrix} \quad \text{(E)}$$

Matrix Representation of Hooke's law for isotropic material

By inverting the above matrix formula so that strains are given explicitly in terms of stresses, we get the compliance matrix from which we can find the elastic constants E,v and G.

$$\begin{bmatrix} \varepsilon_1 \\ \varepsilon_2 \\ \varepsilon_3 \\ \varepsilon_4 \\ \varepsilon_5 \\ \varepsilon_6 \end{bmatrix} = \begin{bmatrix} \frac{1}{E} & -\frac{\nu}{E} & -\frac{\nu}{E} & 0 & 0 & 0 \\ -\frac{\nu}{E} & \frac{1}{E} & -\frac{\nu}{E} & 0 & 0 & 0 \\ -\frac{\nu}{E} & -\frac{\nu}{E} & \frac{1}{E} & 0 & 0 & 0 \\ 0 & 0 & 0 & \frac{1}{2G} & 0 & 0 \\ 0 & 0 & 0 & 0 & \frac{1}{2G} & 0 \\ 0 & 0 & 0 & 0 & 0 & \frac{1}{2G} \end{bmatrix} \begin{bmatrix} \sigma_1 \\ \sigma_2 \\ \sigma_3 \\ \sigma_4 \\ \sigma_5 \\ \sigma_6 \end{bmatrix} \quad \text{(F)}$$

Matrix Representation of Constitutive equation in terms on elastic constants

We'll be analyzing Elastic properties of a Multiferroic composite using Finite Element Method using COMSOL software.

Finite Element Method (FEM)

The Finite Element Method (FEM), is a numerical method that is used for solving problems of Engineering and Mathematical Physics. The finite element method breaks down the problem into a system of algebraic equations. To solve a problem, FEM subdivides a large problem into smaller, simpler parts that are called finite elements. Then it computes approximate values of the unknowns at discrete number of points over the domain.

- Equilibrium equations (they imply that the structure is in equilibrium)
- Compatibility equations (they assume that the structure doesn't fall apart or breaks)
- Force-Displacement equations (they relate displacements to forces, are also called Constitutive relations, e.g Hooke's law)

We'll be doing *displacement method of analysis*, in which the primary unknowns are the displacements. In this method, first the force-displacement relations (Constitutive relations) are computed and subsequently equations satisfying the equilibrium conditions are written. After determining the unknown displacements, the other forces are calculated satisfying the compatibility conditions and force displacement relations. Consider an Aluminum Boron system where Aluminium is the matrix and Boron is the reinforcement. We use Boron as reinforcement as it is hard and hence provides strength to the composite. The volume fraction as well as the aspect ratio of the reinforcement can be varied. I have considered spherical and cylindrical reinforcement. Figure 8.c depicts a cylindrical Boron reinforcement and 8.b depicts spherical Boron reinforcement.

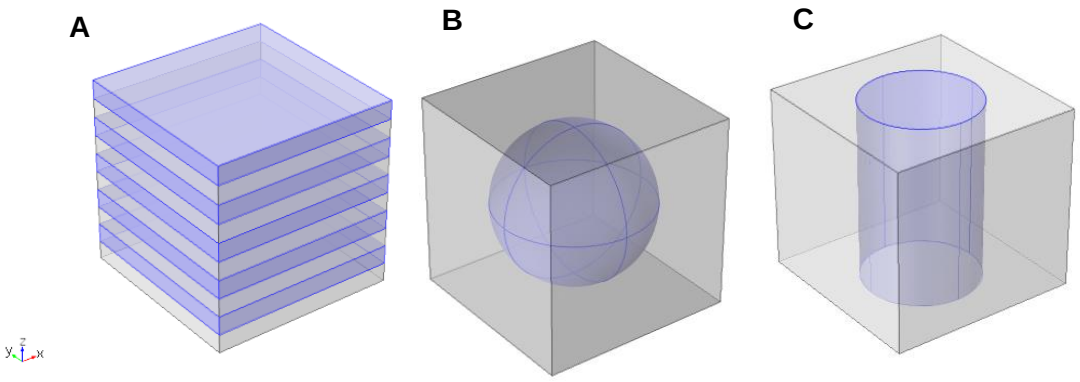

Fig 2.(a) Multilayered reinforcement (b) Spherical Reinforcement (c) Cylindrical Reinforcement

By varying displacement in different directions we calculate stresses developed in the material for all the cases and then calculate the elastic constants. An important thing to note here is that we fix a displacement in one direction while keeping all other displacement values as zero.

In the above figures we can see that the composites are symmetric about the center of cube (origin), therefore during computation we can reduce the calculation to $1/8^{th}$ of the volume to reduce the computation time.

The maximum volume fraction possible for a spherical inclusion is, when the radius of the inclusion is a/2 and that value is $(4\pi(a/2)^3)/(3a^3) = 0.52$.

We define the radius of spherical inclusion as a function of volume fraction and vary the volume fraction from 0.05 to 0.5 with the step size of 0.05 units.

Similarly, maximum volume fraction possible for a cylindrical inclusion is 0.785.
We define the radius of cylindrical inclusion as a function of volume fraction and vary the volume fraction from 0.05 to 0.7 with the step size of 0.05 units and fix the height at 1 unit.
We find C_{11} and C_{12} in both cylindrical and spherical reinforcement by fixing the displacement in x direction as 0.001 units keeping the displacement in all other directions zero. Same way we find C_{22}, C_{23} and C_{33}, C_{13} by fixing displacement in y direction and z direction as 0.001 units respectively keeping displacements in all other directions zero. We find C_{44} by fixing displacement in y direction as y=2*z*0.001, C_{55} by fixing displacement in y direction as y=2*z*0.001 and C_{66} by fixing displacement in y direction as y=2*z*0.001.

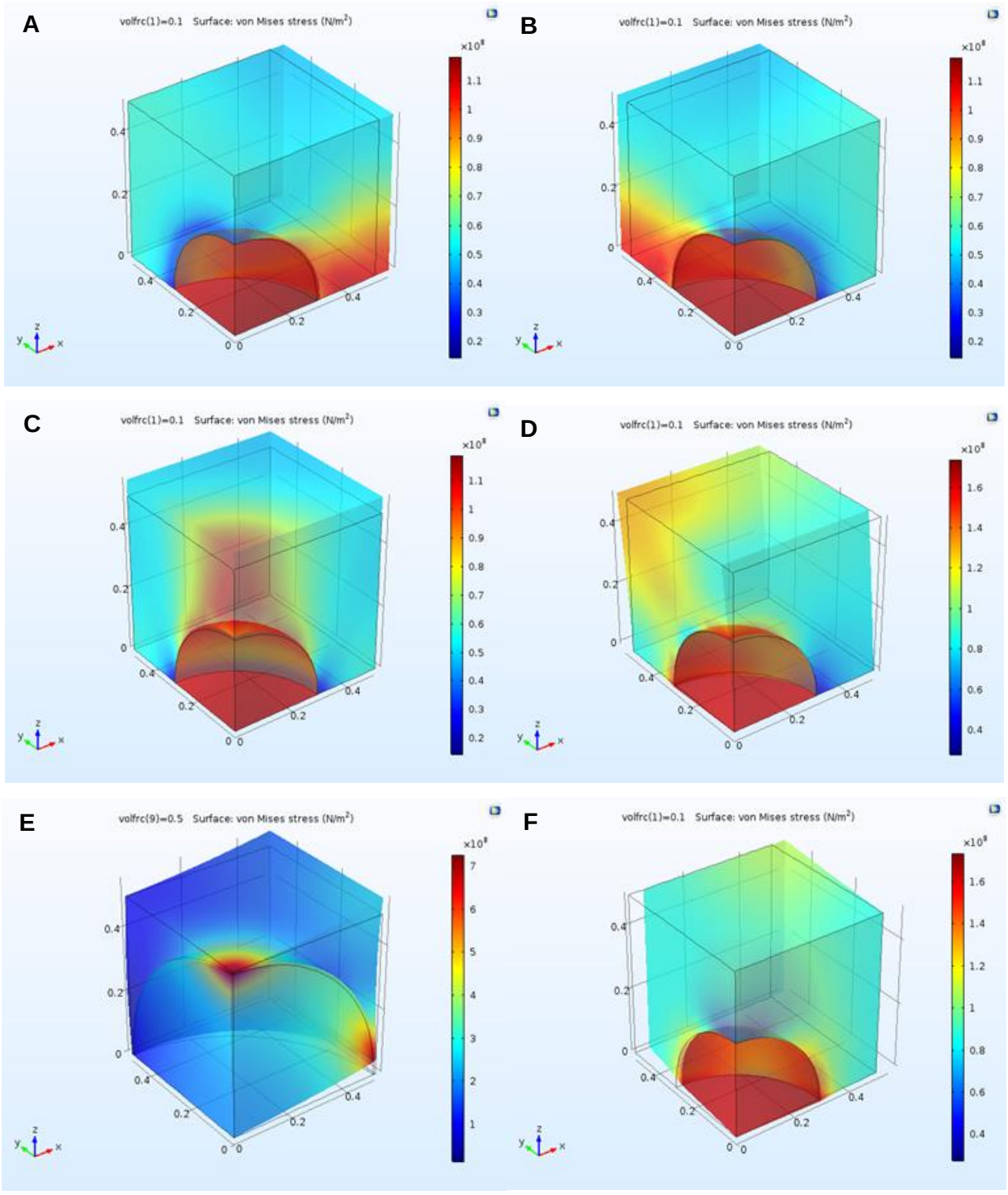

Fig 3.(a) Calculation of C_{11}, C_{12} (b) Calculation of C_{22}, C_{23} (c) Calculation of C_{33}, C_{13} (d) Calculation of C_{44} (e) Calculation of C_{55} (f) Calculation of C_{66}

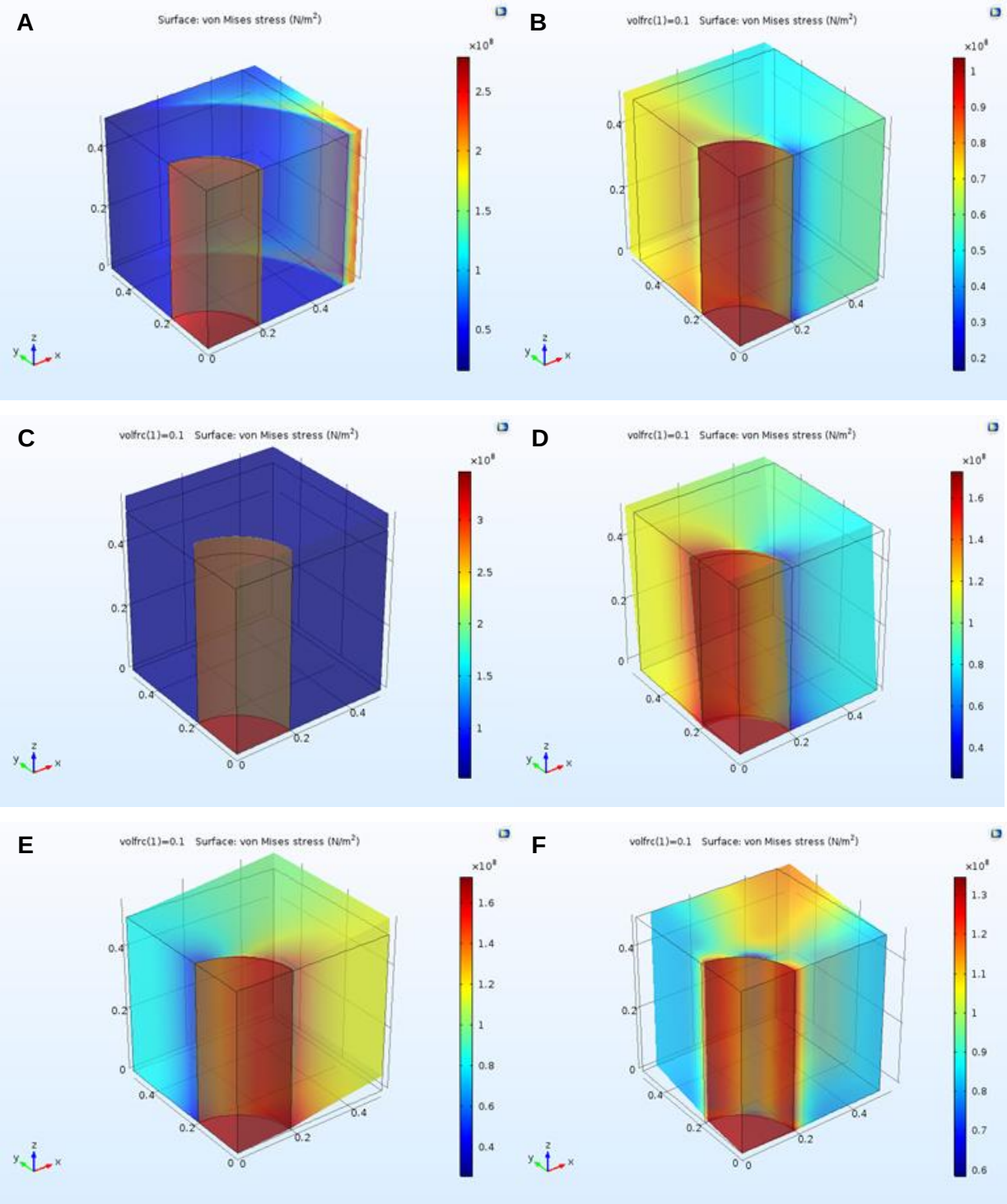

Fig 4.(a) Calculation of C_{11}, C_{12} (b) Calculation of C_{22}, C_{23} (c) Calculation of C_{33}, C_{13} (d) Calculation of C_{44} (e) Calculation of C_{55} (f) Calculation of C_{66}

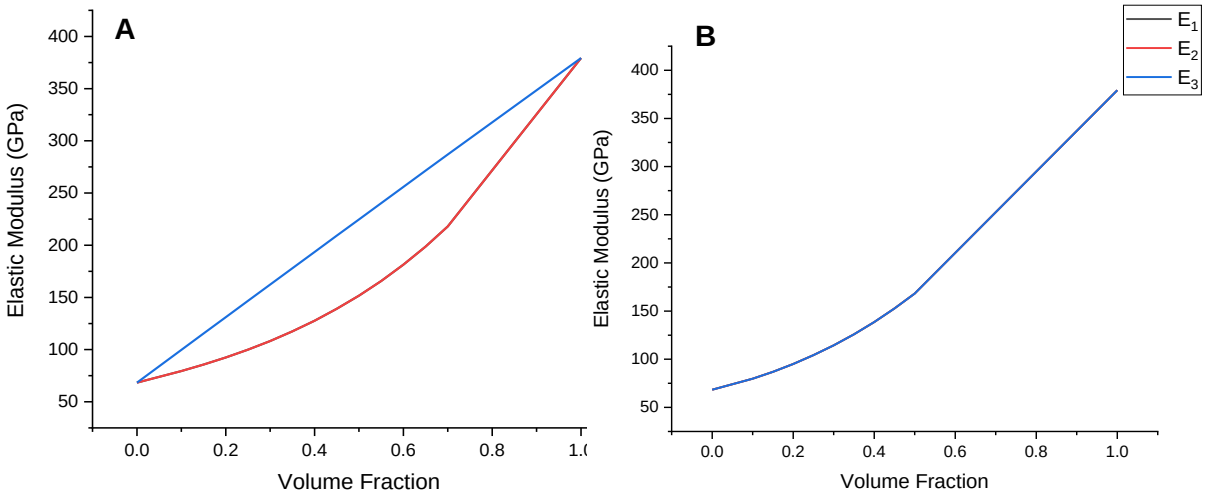

Fig 5. Elastic Modulus Values. (a) Cylindrical Reinforcement (b) Spherical Reinforcement

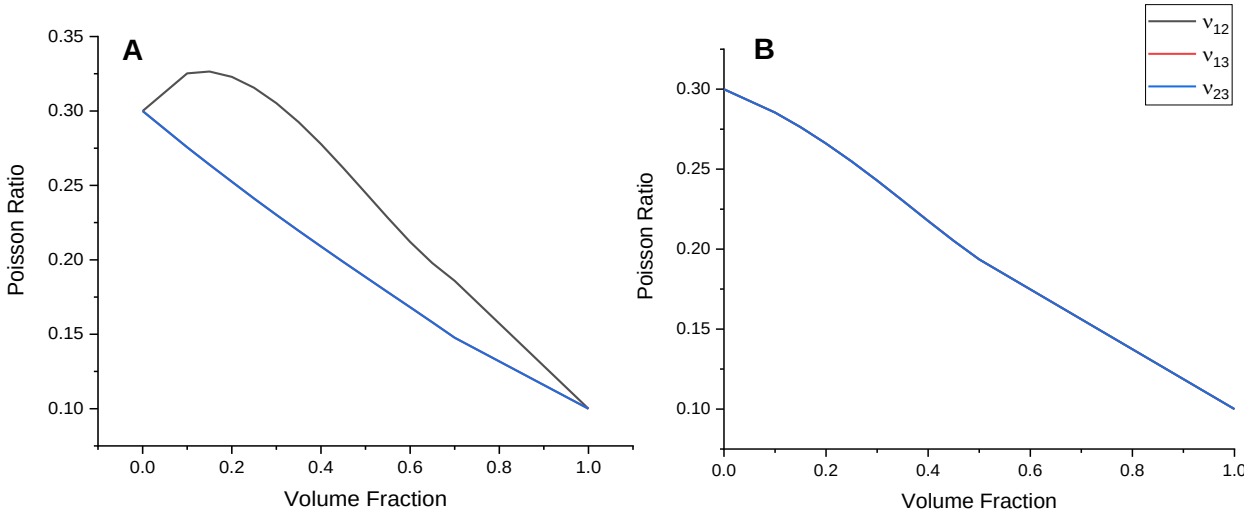

Fig 6. Poisson Ratio Values. (a) Cylindrical Reinforcement (b) Spherical Reinforcement

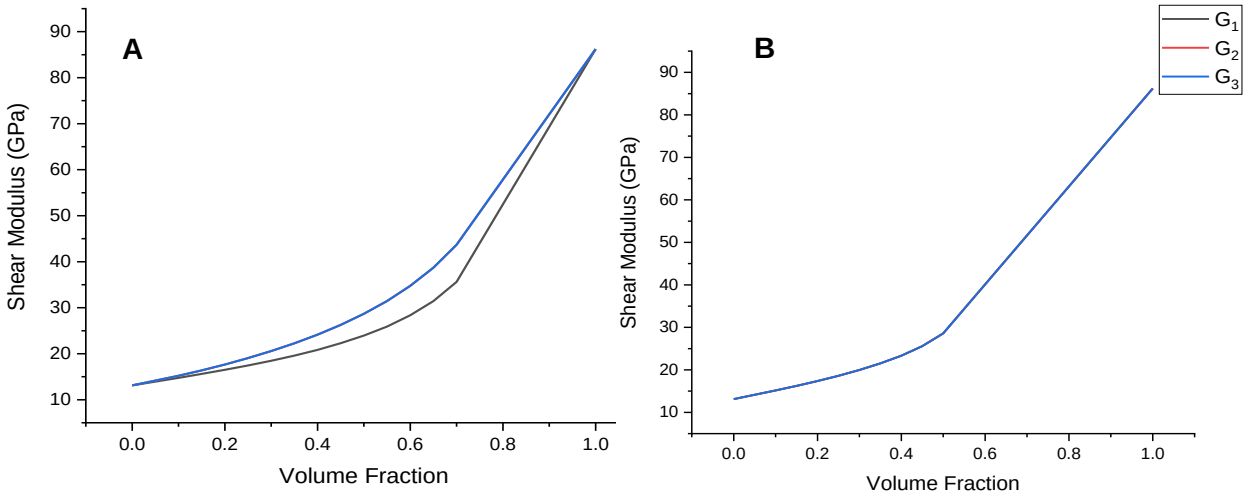

Fig 7. Shear Modulus Values. (a) Cylindrical Reinforcement (b) Spherical Reinforcement

From the graphs as well as the elastic constant values, it can be seen that $E_1=E_2$, $v_{13}=v_{23}$, $G_2=G_3$ in cylindrical reinforcement case which means that the cylindrical reinforcement composite is transversely isotropic and $E_1=E_2=E_3$, $v_{13}=v_{23}=v_{12}$, $G_1=G_2=G_3$ in spherical reinforcement case which means that the spherical reinforcement composite is isotropic.

We carried out similar simulations for SU8 as matrix and Zinc Oxide as reinforcement. For cylindrical reinforcements, the composite formed was again transversely isotropic. Here the elastic properties were only dependent on the amount of strain/stress applies but in piezoelectric, piezomagnetic and multiferroic composites the elastic properties are dependent on several other factors which will be discussed in the next section.

3.2 Piezoelectric Properties

Piezoelectric effect was discovered by Jacques and Pierre Curie in 1888 where they demonstrated that, on application of stress on certain crystalline materials, an electrical charge is produced on the material surface. This was termed as the direct effect. It was later demonstrated that the converse effect is also true; on application of electric field on a piezoelectric material, it changes its shape and size. The reason behind this phenomenon is the specific charge distribution of electric charges inside an unit cell. The piezoelectric effect is only demonstrated in materials with non-centrosymmetric crystal structure. Some of the commonly used/known piezoelectric materials are quartz (SiO_2), zinc oxide (ZnO), polyvinylidenefluoride (PVDF) and lead zirconate titanate, (PZT or $Pb(Zr,Ti)O_3$).

In elastic materials the strain (stress) in the material was only dependent on the stress (strain) applied whereas in piezoelectric materials the strain (stress) is dependent on stress (strain) as well as the electric field (electric displacement).

It was observed that at low stresses and low electric fields, the relation between strain, stress and electric field was linear. If we aasume that the total strain in the material is the sum of mechanical strain induced by mechanical stress and controllable actuation strain caused by the electric field, we can define the constitutive equations as given below,

$$\sigma_{ij} = C_{ijkl}\varepsilon_{ij} - e^{T}_{kij}E_m \qquad (2)\ (3)$$
$$D_m = e_{kij}\varepsilon_{ij} + \kappa_{ij}E_m$$

The piezoelectric coefficient $\mathbf{d_{ij}}$ is the ratio of the strain in the j-axis to the electric field applied along the i-axis, when all other electric fields are zero, electric displacement $\mathbf{D_i}$ is the electric displacement in either in one of the 3 directions (x, y or z), electric field $\mathbf{E_i}$ is the electric field in either in one of the 3 directions (x, y or z), dielectric constant $\mathbf{e_{ij}}$ is the the charge per unit area in the *i*-axis due to an electric field applied in the *j*-axis, when all external stresses are held constant, $\boldsymbol{\sigma_i}$ is the stress in either one of the 3 directions (x, y or z) and elastic compliance constant $\boldsymbol{S_{ij}}$ is the ratio of the strain the in *i*-direction to the stress in the *j*-direction, given that there is no change of stress along the other two directions.

$$\begin{bmatrix}\sigma_{11}\\ \sigma_{22}\\ \sigma_{33}\\ \tau_{23}\\ \tau_{13}\\ \tau_{12}\end{bmatrix} = \begin{bmatrix} C_{11} & C_{21} & C_{31} & C_{41} & C_{51} & C_{61}\\ C_{12} & C_{22} & C_{23} & C_{42} & C_{52} & C_{62}\\ C_{13} & C_{23} & C_{33} & C_{43} & C_{53} & C_{63}\\ C_{14} & C_{24} & C_{34} & C_{44} & C_{54} & C_{64}\\ C_{15} & C_{25} & C_{35} & C_{45} & C_{55} & C_{65}\\ C_{16} & C_{26} & C_{36} & C_{46} & C_{56} & C_{66}\end{bmatrix}\begin{bmatrix}\varepsilon_{11}\\ \varepsilon_{22}\\ \varepsilon_{33}\\ \gamma_{23}\\ \gamma_{13}\\ \gamma_{12}\end{bmatrix} - \begin{bmatrix} e_{11} & e_{21} & e_{31}\\ e_{12} & e_{22} & e_{32}\\ e_{13} & e_{23} & e_{33}\\ e_{14} & e_{24} & e_{34}\\ e_{15} & e_{25} & e_{35}\\ e_{16} & e_{26} & e_{36}\end{bmatrix}\begin{bmatrix}E_1\\ E_2\\ E_3\end{bmatrix} \qquad (G)$$

Matrix Representation of Constitutive equation for direct piezoelectric effect

$$\begin{bmatrix}D_1\\ D_2\\ D_3\end{bmatrix} = \begin{bmatrix} e_{11} & e_{12} & e_{13} & e_{14} & e_{15} & e_{16}\\ e_{21} & e_{22} & e_{23} & e_{24} & e_{25} & e_{26}\\ e_{31} & e_{32} & e_{33} & e_{34} & e_{35} & e_{36}\end{bmatrix}\begin{bmatrix}\varepsilon_{11}\\ \varepsilon_{22}\\ \varepsilon_{33}\\ \gamma_{23}\\ \gamma_{13}\\ \gamma_{12}\end{bmatrix} + \begin{bmatrix} \kappa_{11} & \kappa_{12} & \kappa_{13}\\ \kappa_{21} & \kappa_{22} & \kappa_{23}\\ \kappa_{31} & \kappa_{32} & \kappa_{33}\end{bmatrix}\begin{bmatrix}E_1\\ E_2\\ E_3\end{bmatrix} \qquad (H)$$

Matrix Representation of Constitutive equation for converse piezoelectric effect

We can combine the constitutive equation and express them in matrix form as,

$$\begin{bmatrix} \sigma_{11} \\ \sigma_{22} \\ \sigma_{33} \\ \sigma_{23} \\ \sigma_{13} \\ \sigma_{12} \\ D_1 \\ D_2 \\ D_3 \end{bmatrix} = \begin{bmatrix} C_{11} & C_{12} & C_{13} & C_{14} & C_{15} & C_{16} & e_{11} & e_{21} & e_{31} \\ C_{21} & C_{22} & C_{23} & C_{24} & C_{25} & C_{26} & e_{12} & e_{22} & e_{32} \\ C_{31} & C_{32} & C_{33} & C_{34} & C_{35} & C_{36} & e_{13} & e_{23} & e_{33} \\ C_{41} & C_{42} & C_{43} & C_{44} & C_{45} & C_{46} & e_{14} & e_{24} & e_{34} \\ C_{51} & C_{52} & C_{53} & C_{54} & C_{55} & C_{56} & e_{15} & e_{25} & e_{35} \\ C_{61} & C_{62} & C_{63} & C_{64} & C_{65} & C_{66} & e_{16} & e_{26} & e_{36} \\ e_{11} & e_{12} & e_{13} & e_{14} & e_{15} & e_{16} & -\kappa_{11} & -\kappa_{12} & -\kappa_{13} \\ e_{21} & e_{22} & e_{23} & e_{24} & e_{25} & e_{26} & -\kappa_{21} & -\kappa_{22} & -\kappa_{23} \\ e_{31} & e_{32} & e_{33} & e_{34} & e_{35} & e_{36} & -\kappa_{31} & -\kappa_{32} & -\kappa_{33} \end{bmatrix} \begin{bmatrix} \varepsilon_{11} \\ \varepsilon_{22} \\ \varepsilon_{33} \\ \varepsilon_{23} \\ \varepsilon_{13} \\ \varepsilon_{12} \\ E_1 \\ E_2 \\ E_3 \end{bmatrix} \quad \text{(I)}$$

Electroelastic Matrix

Similar to the elastic material matrix, we can simplify the electroelastic matrix into a much simpler form.

$$\begin{bmatrix} \sigma_{11} \\ \sigma_{22} \\ \sigma_{33} \\ \sigma_{23} \\ \sigma_{13} \\ \sigma_{12} \\ D_1 \\ D_2 \\ D_3 \end{bmatrix} = \begin{bmatrix} C_{11} & C_{12} & C_{13} & 0 & 0 & 0 & 0 & 0 & e_{31} \\ C_{21} & C_{22} & C_{23} & 0 & 0 & 0 & 0 & 0 & e_{32} \\ C_{31} & C_{32} & C_{33} & 0 & 0 & 0 & 0 & 0 & e_{33} \\ 0 & 0 & 0 & C_{44} & 0 & 0 & 0 & e_{24} & 0 \\ 0 & 0 & 0 & 0 & C_{55} & 0 & e_{15} & 0 & 0 \\ 0 & 0 & 0 & 0 & 0 & C_{66} & 0 & 0 & 0 \\ 0 & 0 & 0 & 0 & e_{15} & 0 & -\kappa_{11} & 0 & 0 \\ 0 & 0 & 0 & e_{24} & 0 & 0 & 0 & -\kappa_{22} & 0 \\ e_{31} & e_{32} & e_{33} & 0 & 0 & 0 & 0 & 0 & -\kappa_{33} \end{bmatrix} \begin{bmatrix} \varepsilon_{11} \\ \varepsilon_{22} \\ \varepsilon_{33} \\ \varepsilon_{23} \\ \varepsilon_{13} \\ \varepsilon_{12} \\ E_1 \\ E_2 \\ E_3 \end{bmatrix} \quad \text{(J)}$$

Simplified Electroelastic Matrix

To calculate κ_{11} and e_{15} we fix the electric field in x direction keeping electric fields in all other directions zero. Then we compute σ_{13} to calculate e_{15} and compute D1 to calculate κ_{11}.

Same way we calculate κ_{22}, κ_{33}, e_{24}, e_{31}, e_{32}, e_{33}.

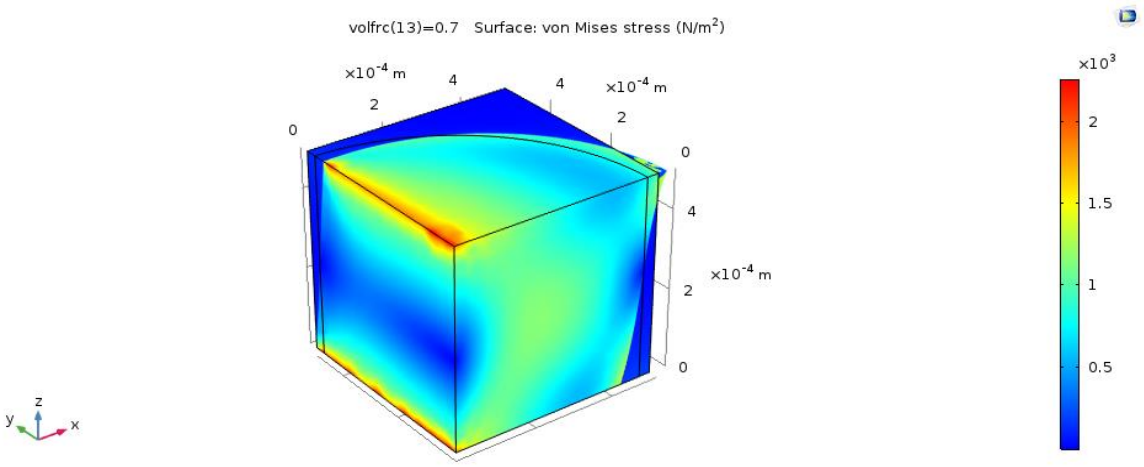

Fig 8. Calculation of κ_{11}, e_{15} for a cylindrical reinforcement

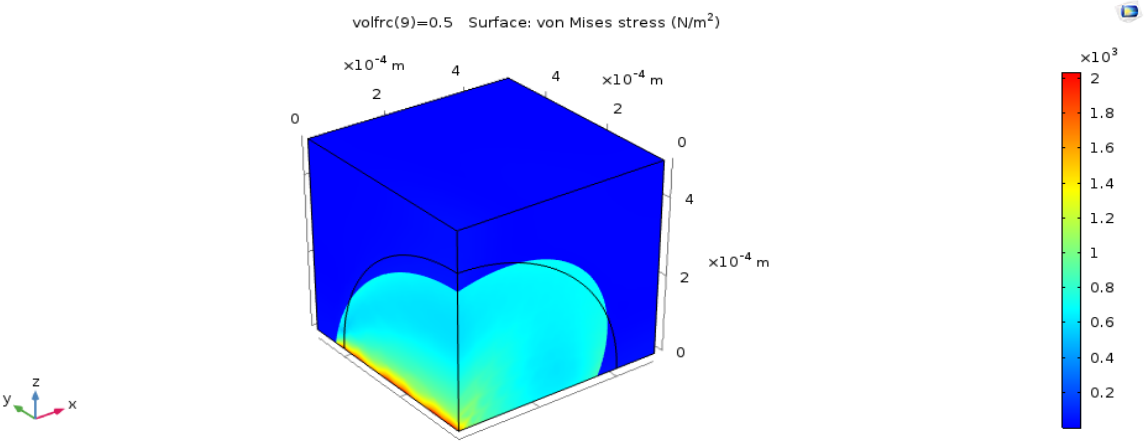

Fig 9. Calculation of κ_{11}, e_{15} for a spherical reinforcement

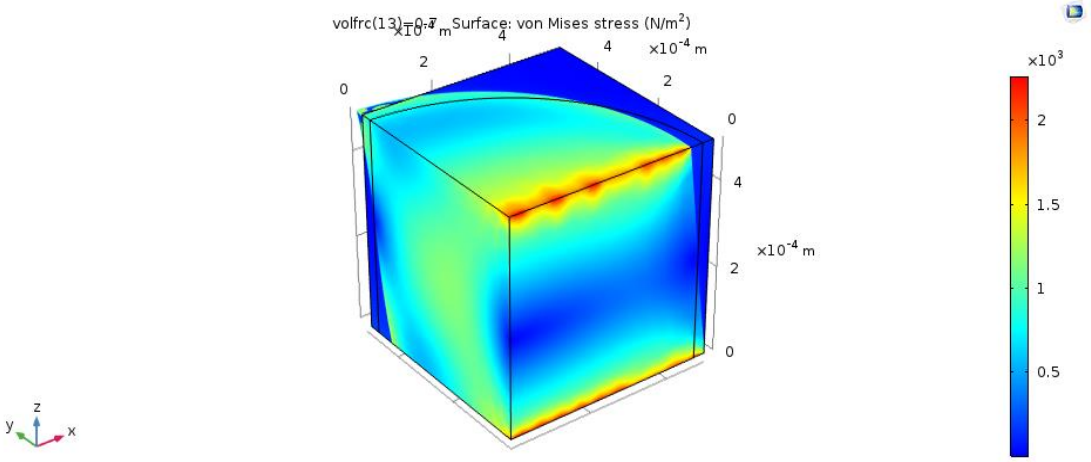

Fig 10. Calculation of κ_{22}, e_{24} for a cylindrical reinforcement

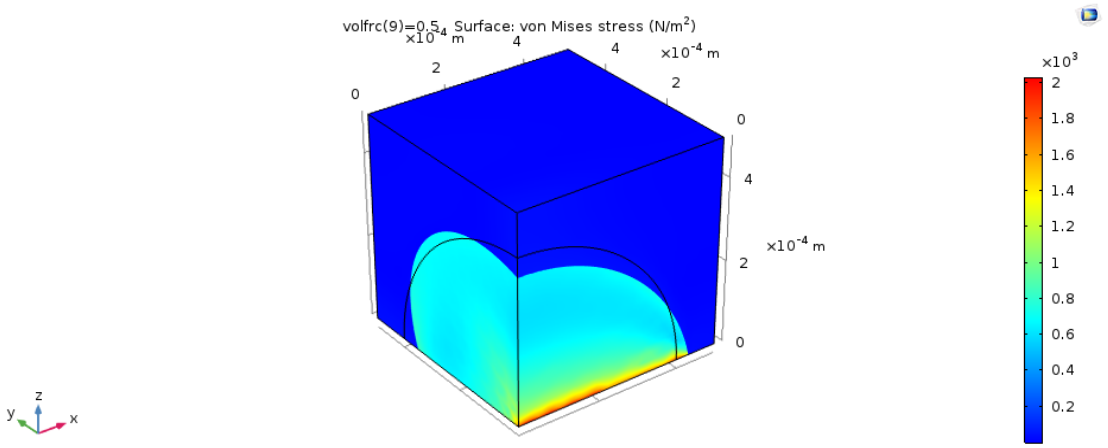

Fig 11. Calculation of κ_{22}, e_{24} for a spherical reinforcement

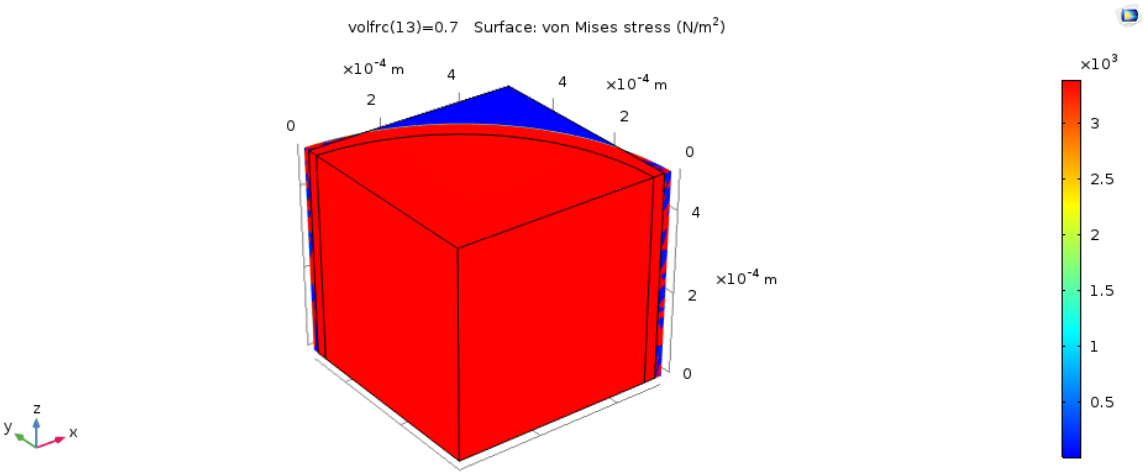

Fig 12. Calculation of κ_{33}, e_{31}, e_{32}, e_{33} for a cylindrical reinforcement

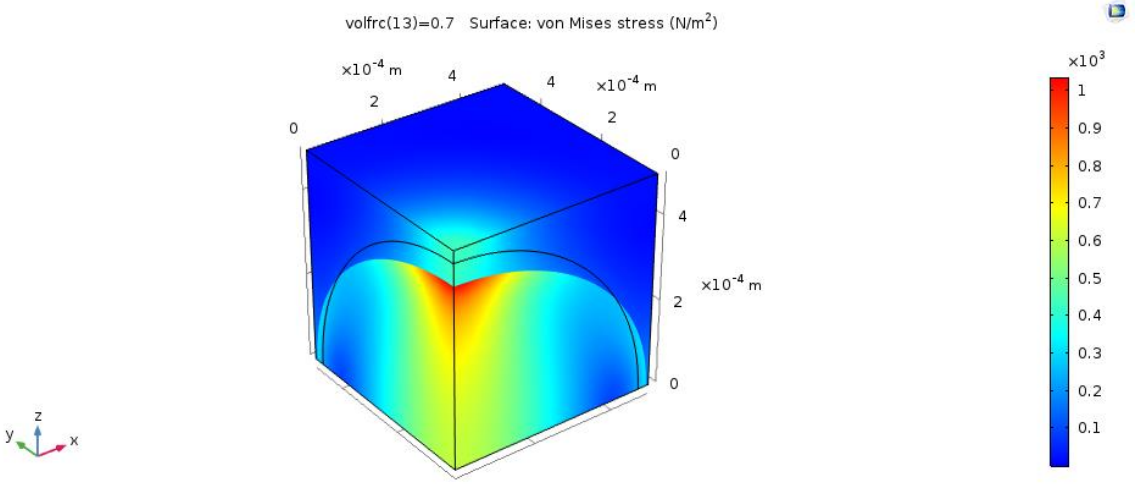

Fig 13. Calculation of κ_{33}, e_{31}, e_{32}, e_{33} for a spherical reinforcement

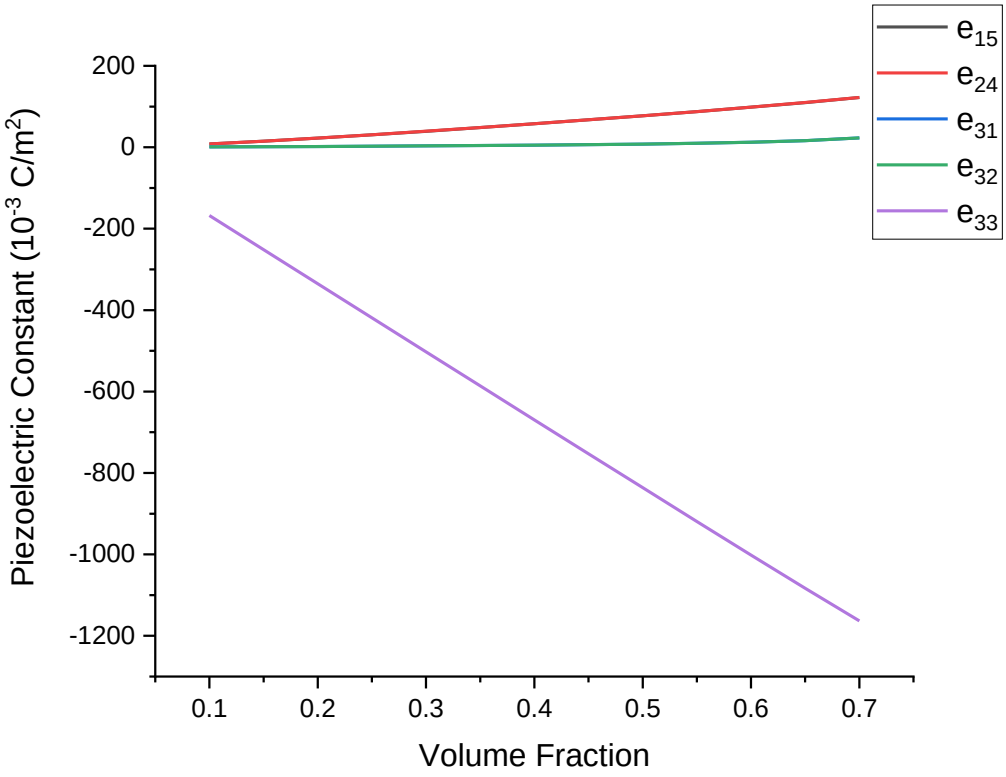

Fig 14. Piezoelectric constants for spherical reinforcement

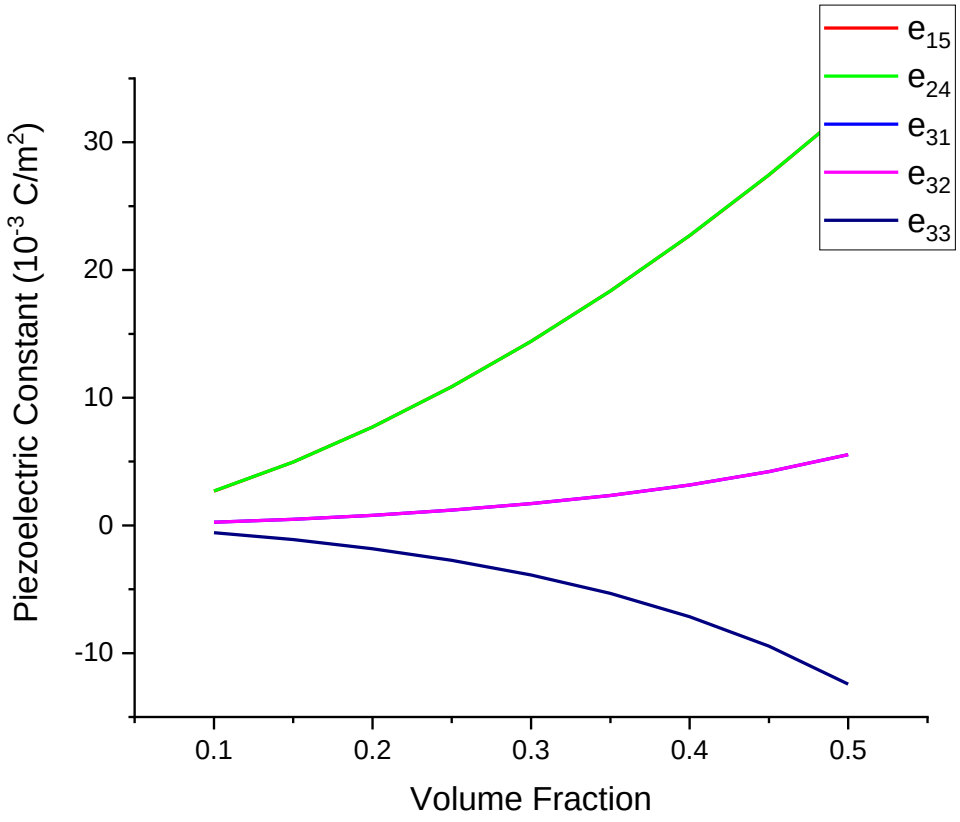

Fig 15. Piezoelectric constants for cylindrical reinforcement

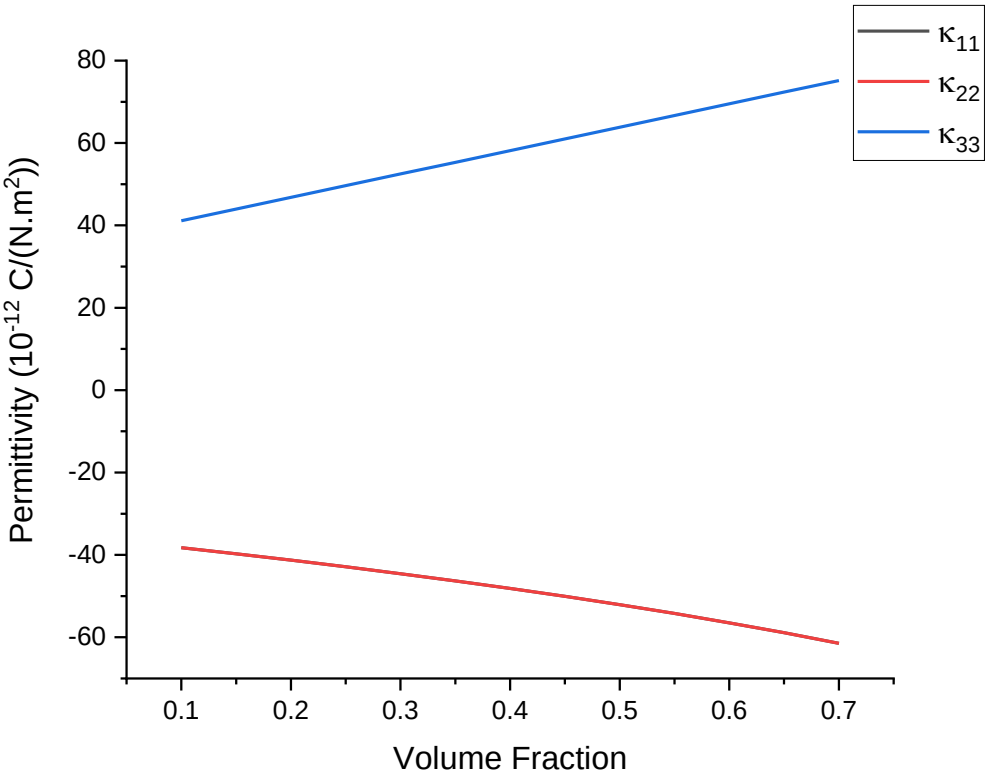

Fig 16. Permittivity constants for spherical reinforcement

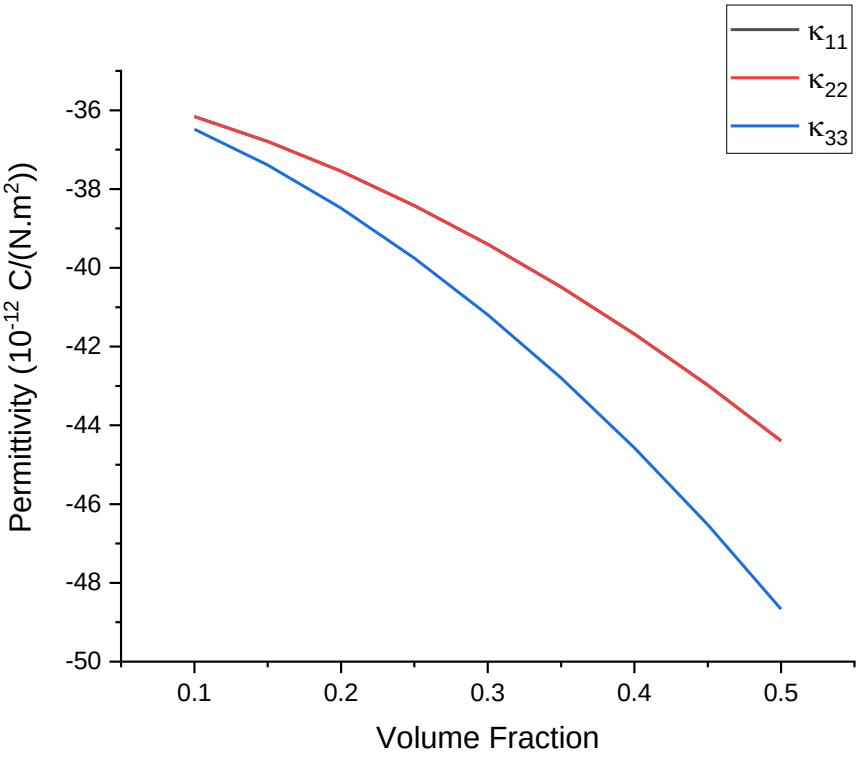

Fig 17. Permittivity constants for cylindrical reinforcement

In the above plot for piezoelectric constant in both spherical as well as the cylindrical reinforcement, we cannot see the e_{15}, and e_{31} values because e_{15} is equal to e_{24} and e_{31} is equal to e_{32}. Similarly we cannot see the κ_{11} in either of the reinforcement because κ_{11} is equal to κ_{22}. The fact that $e_{15}=e_{31}$ and $\kappa_{11}= \kappa_{22}$ are equal proves that the composite if transversely isotropic for both the reinforcements.

3.3 Piezomagnetic Properties

When a magnetic field in applied to a piezomagnetic material, it produces deformation in the material, on the other hand mechanical stress induces change in the magnetic state of the material. Example of a piezomagnetic material is UO_2.

Piezomagnetic materials are characterised by linear coupling between the system's Magnetic Polarisation and Mechanical Strain. In a Piezomagnetic material, we can induce a spontaneous magnetic moment by applying physical stress, or a physical deformation by applying a magnetic field.

Constitutive equation for a piezomagnetic materials are given below,

$$\sigma = C\varepsilon - q^T H \tag{4}$$

$$B = q\varepsilon + \mu H \tag{5}$$

Chapter 4 Magneto electric properties

The piezoelectric and piezomagnetic phase have their usual electrolelastic and magnetoelastic coupling but neither of them have magnetoelctric coupling. But when a composite is prepared using piezoelctric and piezomagentic material as phase and inclusion and vice versa we see that the composite has all the above properties.
The constitutive equation for a multiferroic composite are given below,

$$\sigma = C\varepsilon - e^T E - q^T H,$$
$$D = e\varepsilon + \kappa E + \alpha H, \qquad \text{(6) (7) (8)}$$
$$B = q\varepsilon + \alpha E + \mu H$$

By combining the constitutive equations and expressing them in matrix form gives us,

$$\begin{bmatrix} \sigma \\ D \\ B \end{bmatrix}_{12x1} = [L]_{12x12} \begin{bmatrix} \varepsilon \\ E \\ H \end{bmatrix}_{12x1} \qquad \text{(K)}$$

where L is referred to as the magento-electro-elastic matrix.

$$L = \begin{bmatrix} C & e^T & q^T \\ e & -\kappa & -\alpha \\ q & -\alpha & -\mu \end{bmatrix} \qquad \text{(L)}$$

Assuming that the composite is transversely isotropic, magento-electro-elastic matrix can be simplified to a much simpler form given below.

$$L=\begin{bmatrix} C_{11} & C_{12} & C_{13} & 0 & 0 & 0 & 0 & 0 & e_{31} & 0 & 0 & q_{31} \\ C_{12} & C_{11} & C_{13} & 0 & 0 & 0 & 0 & 0 & e_{31} & 0 & 0 & q_{31} \\ C_{13} & C_{13} & C_{33} & 0 & 0 & 0 & 0 & 0 & e_{33} & 0 & 0 & q_{33} \\ 0 & 0 & 0 & C_{44} & 0 & 0 & 0 & e_{15} & 0 & 0 & q_{15} & 0 \\ 0 & 0 & 0 & 0 & C_{44} & 0 & e_{15} & 0 & 0 & q_{15} & 0 & 0 \\ 0 & 0 & 0 & 0 & 0 & C_{66} & 0 & 0 & 0 & 0 & 0 & 0 \\ 0 & 0 & 0 & 0 & e_{15} & 0 & -\kappa_{11} & 0 & 0 & -\alpha_{11} & 0 & 0 \\ 0 & 0 & 0 & e_{15} & 0 & 0 & 0 & -\kappa_{11} & 0 & 0 & -\alpha_{11} & 0 \\ e_{31} & e_{31} & e_{33} & 0 & 0 & 0 & 0 & 0 & -\kappa_{33} & 0 & 0 & -\alpha_{33} \\ 0 & 0 & 0 & 0 & q_{15} & 0 & -\alpha_{11} & 0 & 0 & -\mu_{11} & 0 & 0 \\ 0 & 0 & 0 & q_{15} & 0 & 0 & 0 & -\alpha_{11} & 0 & 0 & -\mu_{11} & 0 \\ q_{31} & q_{31} & q_{33} & 0 & 0 & 0 & 0 & 0 & -\alpha_{33} & 0 & 0 & -\mu_{33} \end{bmatrix} \quad \text{(M)}$$

Simplified Magneto-electro-elastic matrix

The matrix has 17 independent material constants out of which 5 are elastic ones (C_{11}, C_{12}, C_{13}, C_{33}, C_{44}), 2 are dielectric constants (κ_{11}, κ_{33}), 3 piezoelectric ones (e_{31}, e_{33}, e_{15}), 3 piezomagnetic ones (q_{31}, q_{33}, q_{15}) and 2 magnetoelectric ones (α_{11}, α_{33}).

When we consider a piezoelectric phase, all the pieozmagnetic constants are zero as weee as the magneto electric constants are also zero. Same happens when we consider a piezomagnetic phase, all the piezoelectric constants are zero as well as the magnetoelctric constants are also zero.

We'll be using Mori-Tanaka method to find an effective Magneto-Electro-Elastic Tensor and further find the effective properties from the matrix.

We'll take inclusions as phase 1 and matrix as phase 0, their volume concentrations as c_1 and c_0 and their Magneto-Electro-Elastic Tensor as L_1 and L_0.

We'll be considering 2 composites, on with BTO in CFO and other with CFO in BTO.

The interface between matrix and inclusion can be perfect or imperfect and based on that the equation to find the effective magento-electro-elastic matrix of the composite changes.

For Perfect Interface:

$$L = L_0 + c_1(L_1 - L_0)[I + c_0 S L_0^{-1}(L_1 - L_0)]^{-1} \quad (9)$$

In the above equation S is the Eshelby's S tensor of the ellipsoid inclusion in the matrix phase which can be piezoelectric or piezomagentic. The above equation can be written explicitly only for fibrous and multi-layered composite and can be evaluated numerically for all other aspect ratios.

In case of an imperfect interface we assume there exists a thin layer on the surface of the inclusion. Together the coating and the inclusion form a thinly coated inclusion. The volume concentration of the coated inclusion is denoted as c_{int} and volume concentration of the remaining inclusion becomes $(1-c_{int})$.

The magneto-electro-elastic matrix of coated inclusion is given as L_{int} where

$$L_{\text{int}} = [C_{11}^{\text{int}}, C_{44}^{\text{int}}, \kappa^{\text{int}}, \mu^{\text{int}}]$$

Because of the amorphous nature of the interface, it is assumed to be isotropic with piezoelectric, peizomagnetic and magentoelctric constants to be zero.

Assuming the interface as the matrix phase in the thinly coated inclusion, we can rewrite the perfect interface equation by replacing the L with L_{coat} and L_0 with L_{int}.

After finding L_{coat}, we replace the inclusion Magneto-Electro-Elastic matrix, L_1 with L_{coat} in the perfect interface equation. The imperfect interface condition equations mentioned below can be evaluated only for multi-layered and fibrous composite.

$$\begin{aligned} L_{coat} &= L_{\text{int}} + (1 - c_{\text{int}})(L_1 - L_{\text{int}})[I + c_{\text{int}} S L_{\text{int}}^{-1}(L_1 - L_{\text{int}})]^{-1} \\ L &= L_0 + c_1(L_{coat} - L_0)[I + c_0 S L_0^{-1}(L_{coat} - L_0)]^{-1} \end{aligned} \quad (10)$$

The interface properties for the above equation are taken from Wang et al. (205) and they are,

$C_{11}^{\text{int}} = 3*10^9\, Pa; C_{44}^{\text{int}} = 1*10^9\, Pa; \kappa^{\text{int}} = 2\varepsilon_0; \mu^{\text{int}} = 2\mu_0$,where μ_0 is vacuum permeability and ε_0 is vacuum permittivity.

The initial volume concentration of the interface c_{int} is taken as 0.01 (1% of the coated inclusion) and is assumed to be reduced to zero as c_1 reaches 1.
Therefore we assume c_{int} =0.01*[1-F(c_1;20,1)] where, F is the cumulative distribution of the Beta function. The beta distribution is a family of continuous probability distributions defined on the interval [0, 1] which is parametrized by two positive shape parameters, denoted by α and β, that control the shape of the distribution.

Chapter 5 Results

5.1 Perfect Interface

5.1.1 Magneto electric Coupling coefficients α_{11}, α_{33}

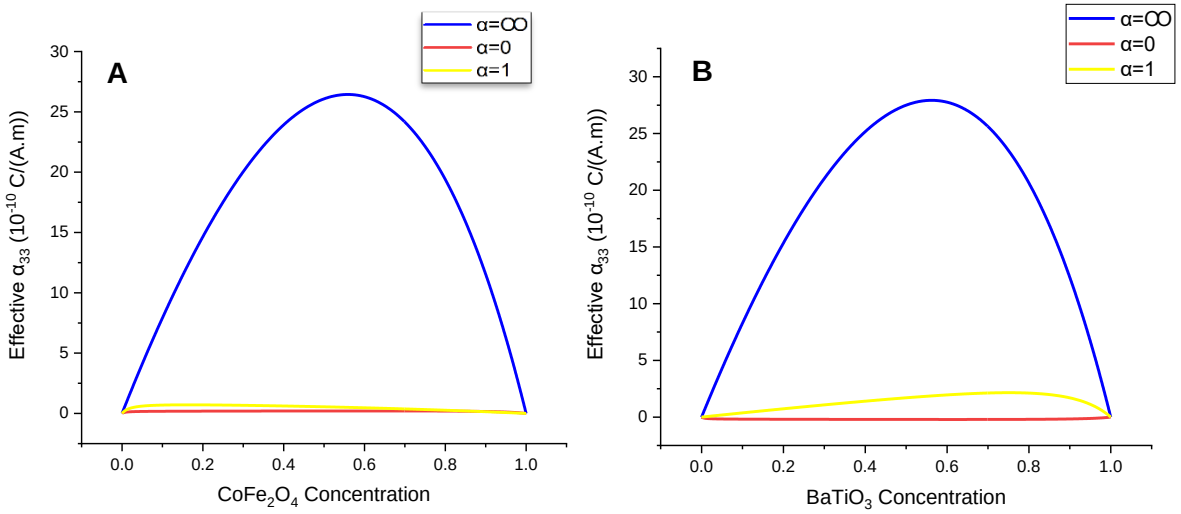

Fig 18. Magneto electric Coupling Coefficient α_{33} (a) CFO-in-BTO (b) BTO-in-CFO

The magneto electric coefficient In the axial direction, α_{33} is shown in Fig 18(a),(b) for CFO-in-BTO and BTO-in-CFO, respectively. We see that the maximum value of magneto electric coupling coefficient is achieved in a fibrous composite ($\alpha=\infty$) in both the cases, BTO-in-CFO and CFO-in-BTO. The magneto electric coupling coefficient value in a multilayered composite ($\alpha=0$) is almost zero for both the cases, BTO-in-CFO and CFO-in-BTO. But for a particulate composite ($\alpha=1$), BTO-in-CFO has a some positive value for higher concentration of $BaTiO_3$ compared to CFO-in-BTO composite for which the value is zero for all concentrations of $CoFe_2O_4$.

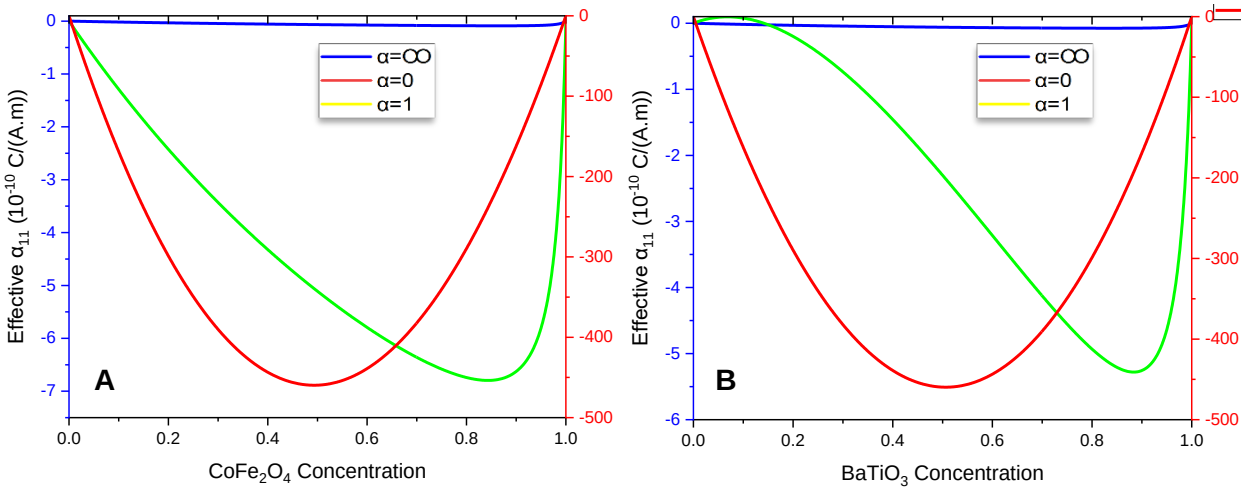

Fig 19. Magneto electric Coupling Coefficient α_{11} (a) CFO-in-BTO (b) BTO-in-CFO

The magneto electric coefficient In the traverse direction, α_{11} is shown in Fig 19(a),(b) for CFO-in-BTO and BTO-in-CFO, respectively. The negative value of α_{11} means that a positive electric field E_1 will generate a negative B_1 value, or conversely a positive magnetic field H_1 will generate a negative D_1 value. In contrast to α_{33}, α_{11} achieved a maximum value in a multilayered composite (α=0) as well as in a particulate composite (α=1) but at different concentrations in both the cases, CFO-in-BTO and BTO-in-CFO. The maximum value of Magneto electric Coupling Coefficient α_{11}, is 10 times more than the maximum value of α_{33} in both the cases. Compared to α_{33}, α_{11} achieved a value close to almost zero in fibrous composite (α=∞) for both the cases, CFO-in-BTO and BTO-in-CFO.

5.1.2 Piezoelectric coefficients e_{15}, e_{31}, e_{33}

The piezoelectric constants e_{ij} connects the applied electric field E_j to the induced mechanical stress σ_i, or conversely the applied mechanical strain ε_j to the induced electric displacement D_i. The variations of these values are plotted against inclusion concentrations and 3 different aspect ratios in Fig. 20, 21 and 22. Since CFO possesses no piezoelectric effect the range of the piezoelectric constants of the composite vary from 0 to the value of BTO. Since value of piezoelectric constant e_{31} is negative for BTO, the value is negative for the composite as well.

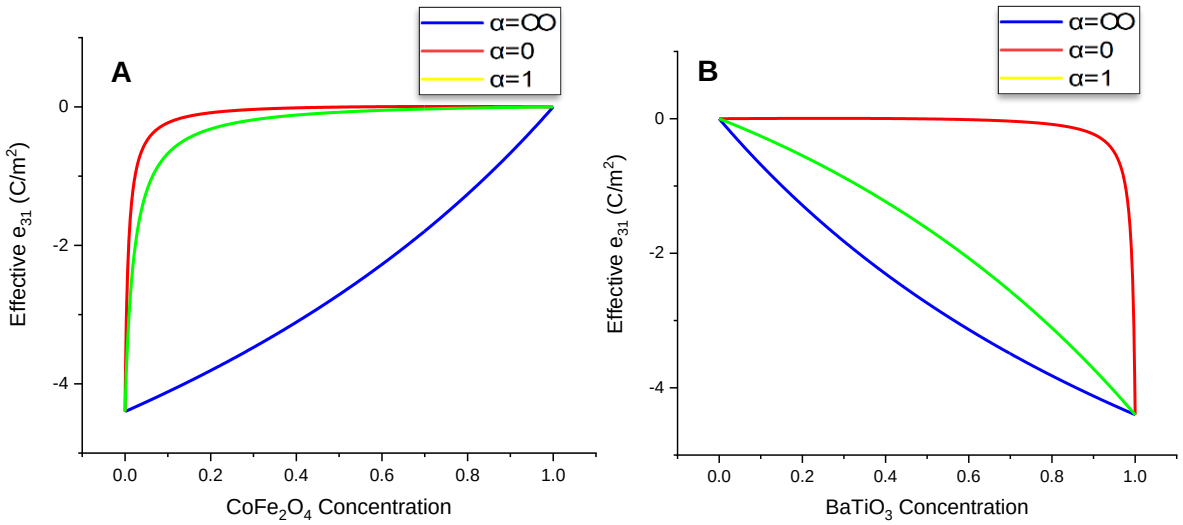

Fig 20. Piezoelectric Constant e_{31} (a) CFO-in-BTO (b) BTO-in-CFO

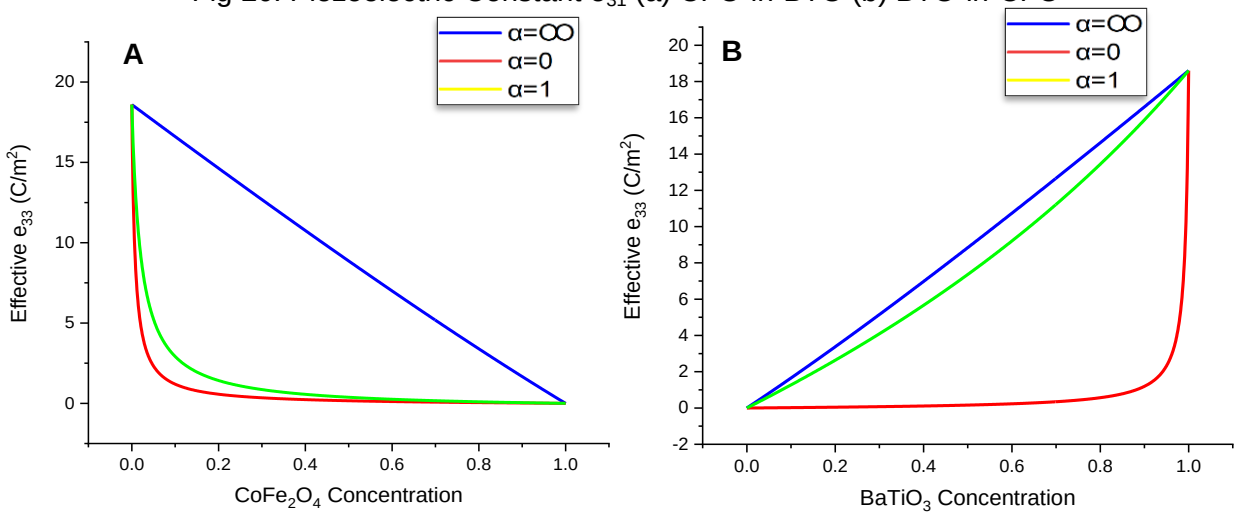

Fig 21. Piezoelectric Constant e_{33} (a) CFO-in-BTO (b) BTO-in-CFO

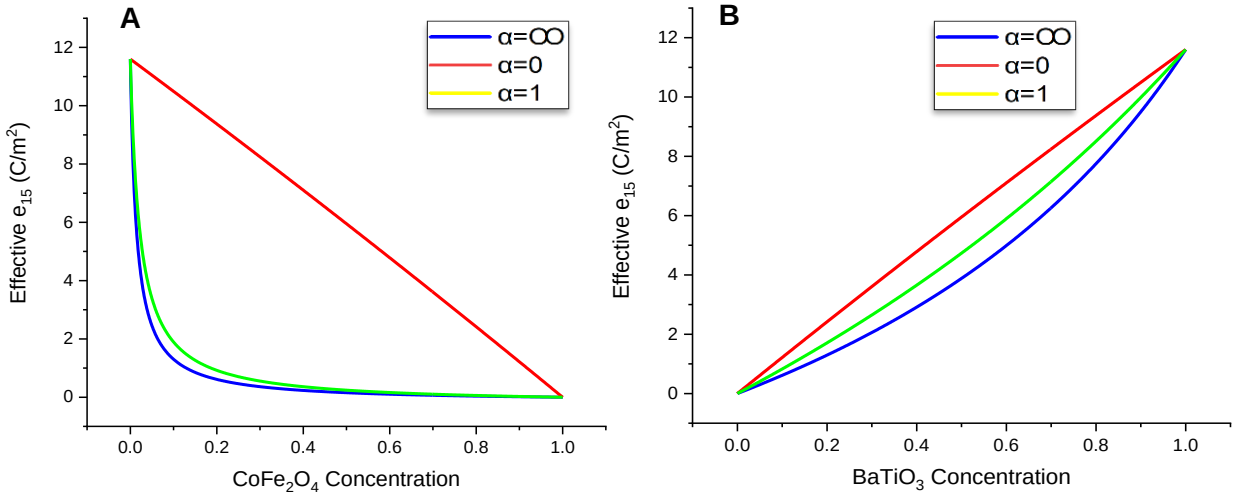

Fig 22. Piezoelectric Constant e_{15} (a) CFO-in-BTO (b) BTO-in-CFO

5.1.3 Piezomagnetic coefficients q_{15}, q_{31}, q_{33}

The piezomagnetic constant q_{31} connects the applied tensile strain ε_1 to the induced magnetic flux density B_3 in the axial direction, or conversely the induced transverse stress σ_1 by the axial magnetic field H_3. Similar is the case for q_{33}. The piezomagnetic constant q_{15} connects the transverse magnetic field H_1 to the induced axial stress σ_5, or conversely axial shear strain ε_5 to the transverse magnetic field H_1 .The variations of these values are plotted against inclusion concentrations and 3 different aspect ratios in Fig. 23, 24 and 25. Since BTO possesses no piezomagnetic effect the range of the piezomagnetic constants of the composite vary from 0 to the value of CFO.

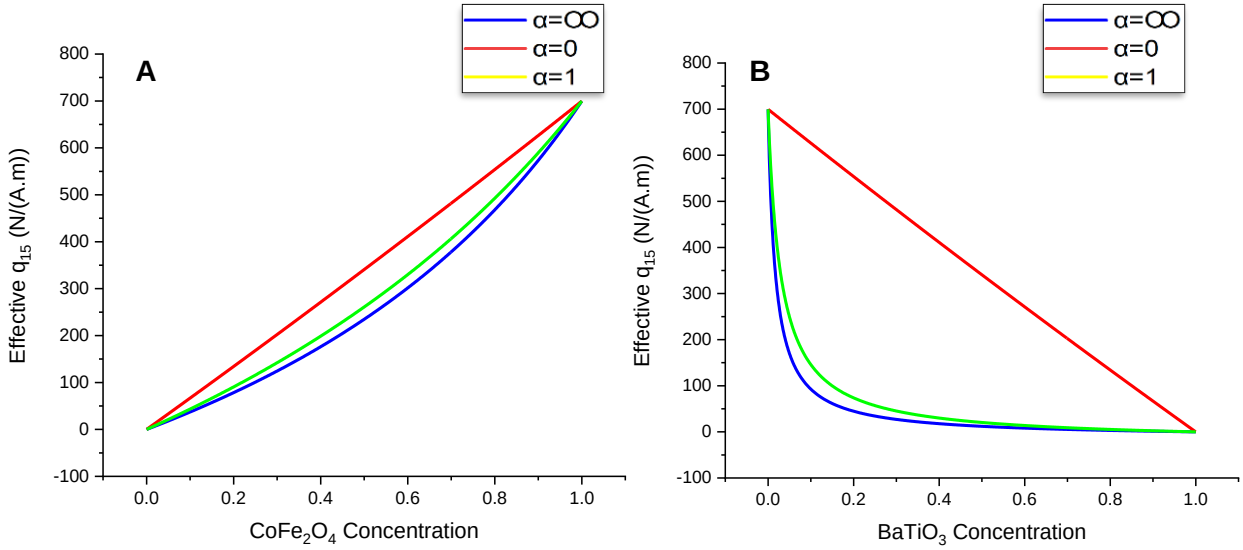

Fig 23. Piezomagnetic Constant q_{15} (a) CFO-in-BTO (b) BTO-in-CFO

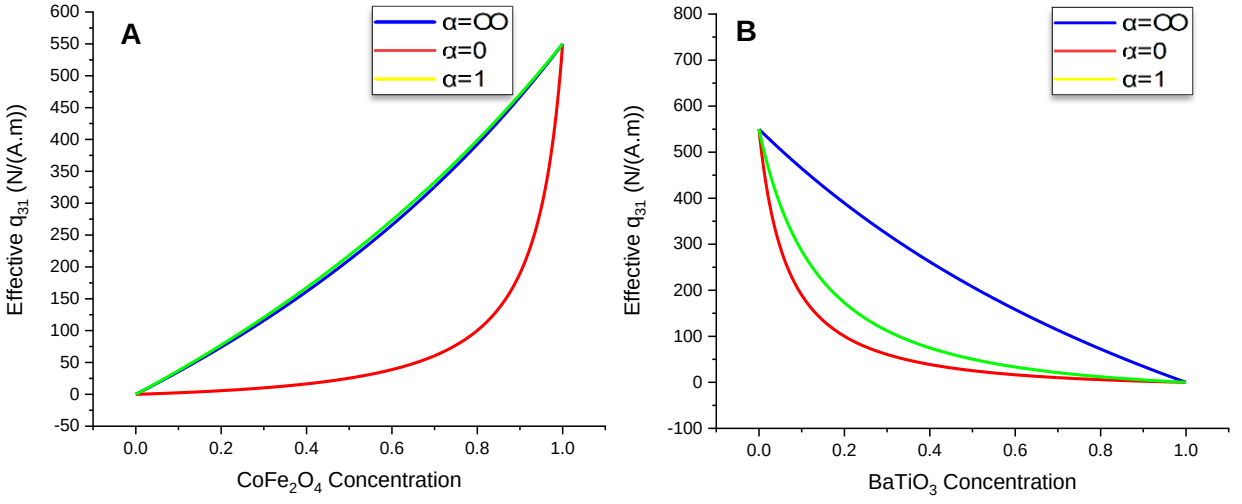

Fig 24. Piezomagnetic Constant q_{31} (a) CFO-in-BTO (b) BTO-in-CFO

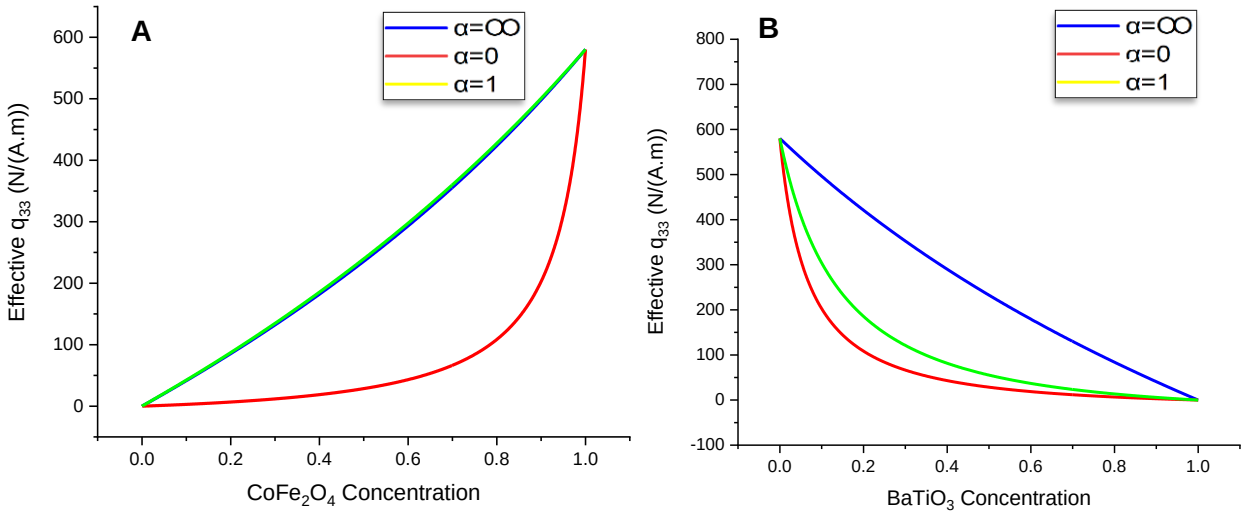

Fig 25. Piezomagnetic Constant q_{33} (a) CFO-in-BTO (b) BTO-in-CFO

5.1.4 Electric Permittivity κ_{11}, κ_{33}

The electric permittivity κ_{33} defines the induced electric displacement, B_3 in the axial direction by the axial electric filed E_3. Same is the case for the κ_{11}, where it connects the induced electric displacement, B_1 in the transverse direction by the transverse electric filed E_1. Since the electric permittivity is strong in BTO and very low in CFO, the plots of κ_{33} and κ_{11} are similar to e_{33} and e_{15} respectively. The variations of these values are plotted against inclusion concentrations and 3 different aspect ratios in Fig. 26 and 27.

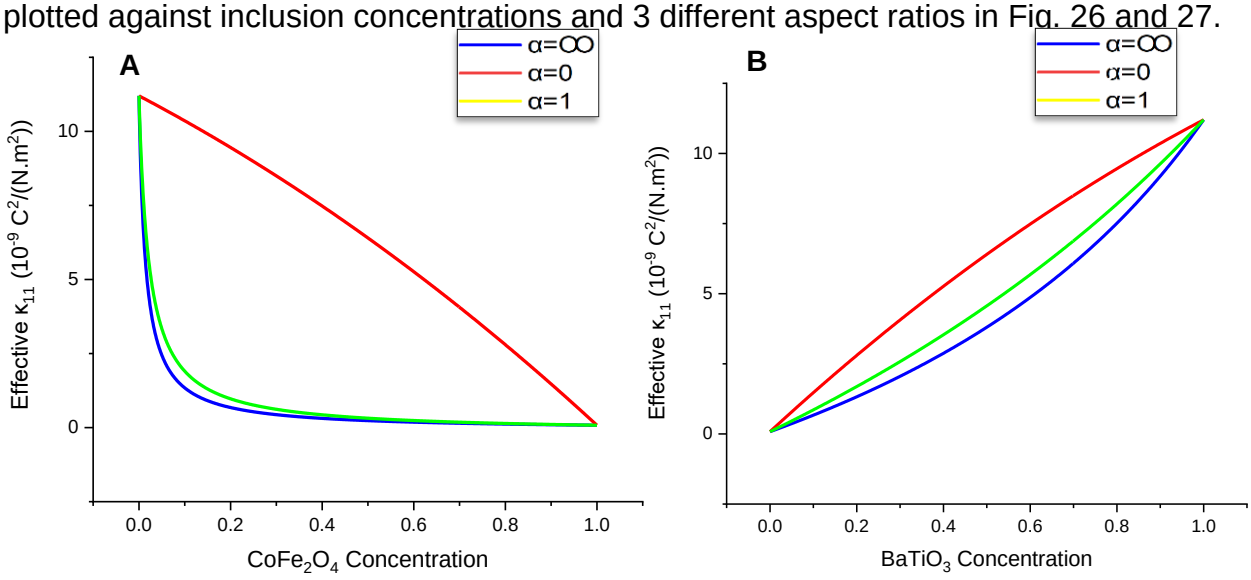

Fig 26. Electric Permittivity κ_{11} (a) CFO-in-BTO (b) BTO-in-CFO

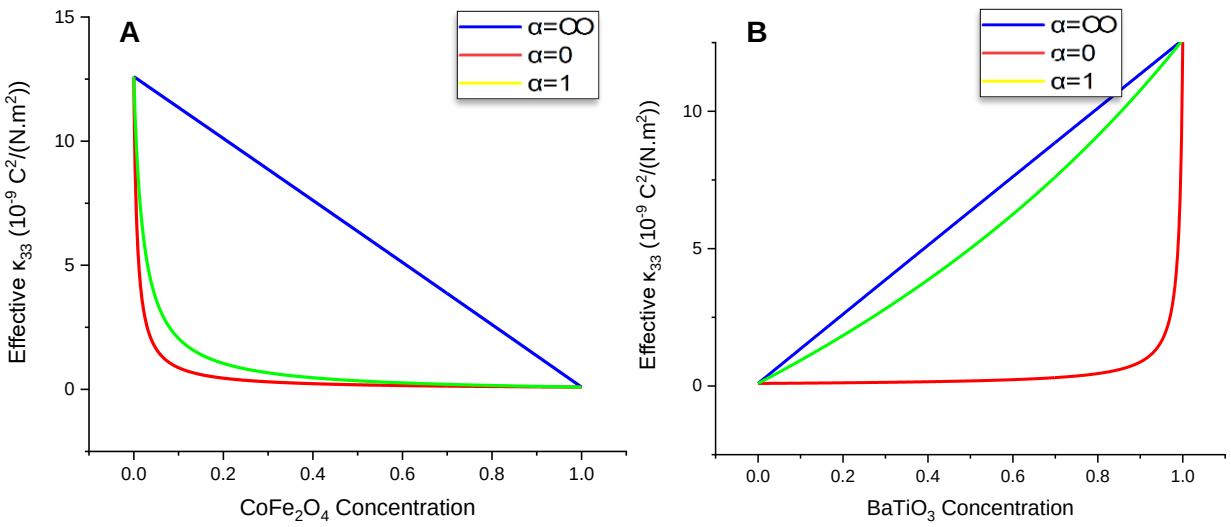

Fig 27. Electric Permittivity κ_{33} (a) CFO-in-BTO (b) BTO-in-CFO

5.1.5 Magnetic Permeability μ_{11}, μ_{33}

The magnetic permeability μ_{33} defines the induced magnetic flux density B_3 in the axial direction by the axial magnetic field H_3. Same is the case for the κ_{11}, where it connects the induced magnetic flux density, B_1 in the transverse direction by the transverse magnetic field H_1.The variations of these values are plotted against inclusion concentration and 3 different aspect ratios in Fig. 28 and 29.

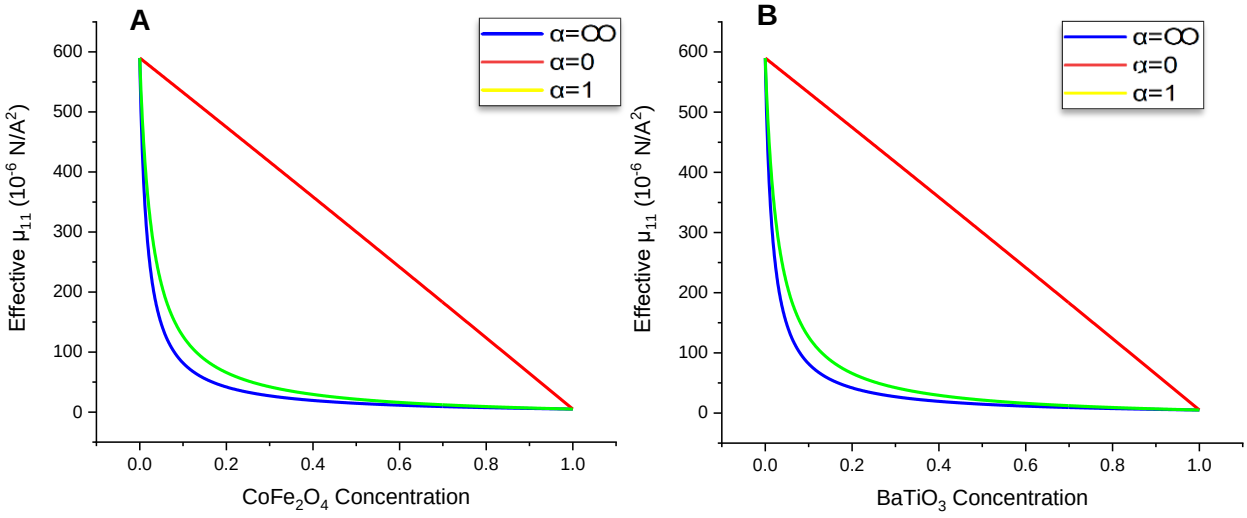

Fig 28. Magnetic Permeability μ_{11} (a) CFO-in-BTO (b) BTO-in-CFO

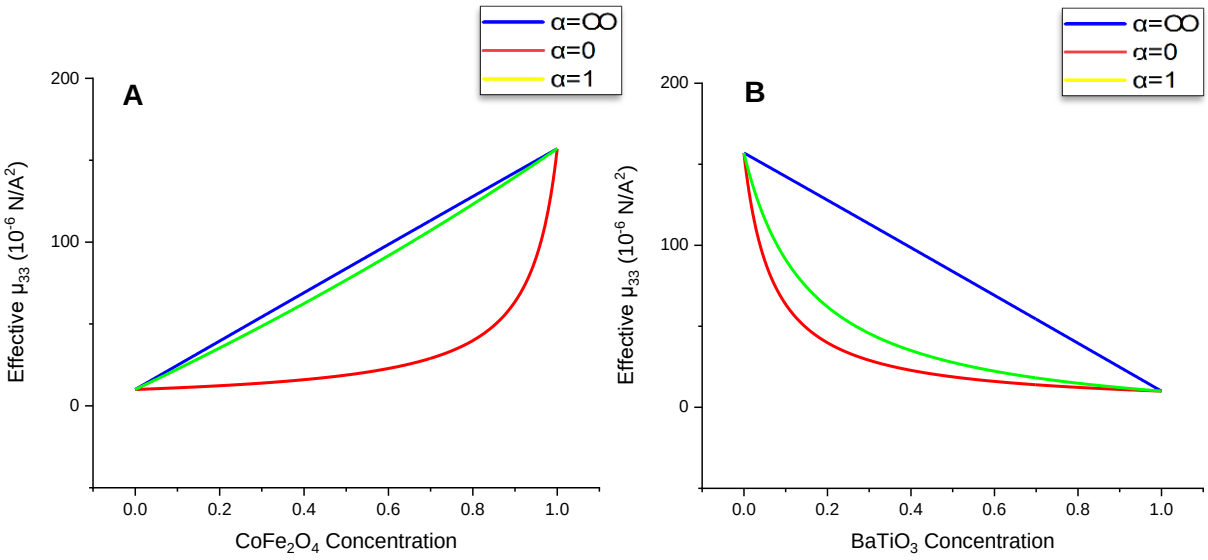

Fig 29. Magnetic Permeability μ_{33} (a) CFO-in-BTO (b) BTO-in-CFO

5.1.6 Elastic Constants C_{11}, C_{12}, C_{13}, C_{33}, C_{44}

The elastic properties of CFO are stiffer than those of BTO which can be seen as an increasing trend for CFO-in-BTO, and a decreasing trend for BTO-in-CFO. There is no dependence of aspect ratio on elastic constants, C_{11}, C_{12} and C_{13} and a slight dependence on C_{33}. But in C_{44}, it can be clearly seen that the elastic constant depends on the aspect ratio. The value of C_{44} is maximum in fibrous composite (α=∞) for both the cases, CFO-in-BTO and BTO-in-CFO and also, the value of C_{44} in fibrous composite (α=∞) for all inlcusion concentrations is more than that in particulate composite (α=1) which is more than that in multilayered composite (α=0) for both the cases, BTO-in-CFO and CFO-in-BTO.

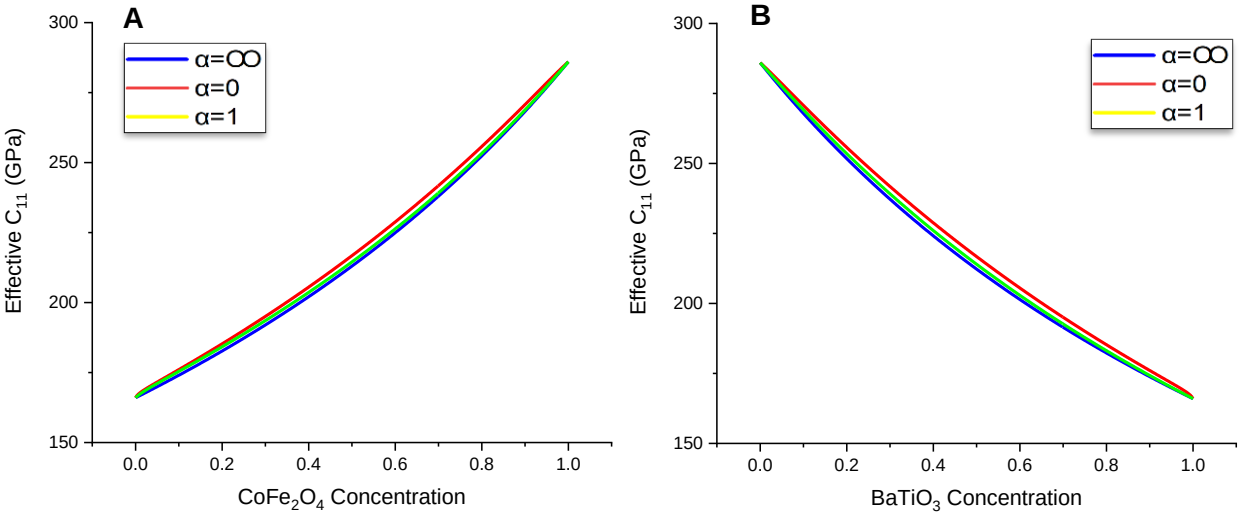

Fig 30. Elastic Constant C_{11} (a) CFO-in-BTO (b) BTO-in-CFO

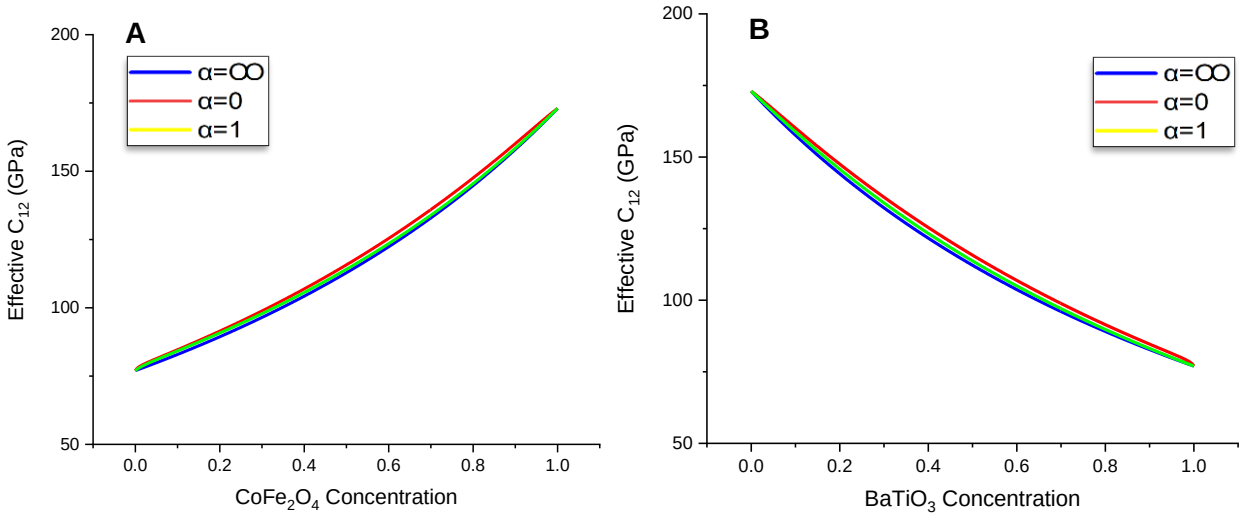

Fig 31. Elastic Constant C_{12} (a) CFO-in-BTO (b) BTO-in-CFO

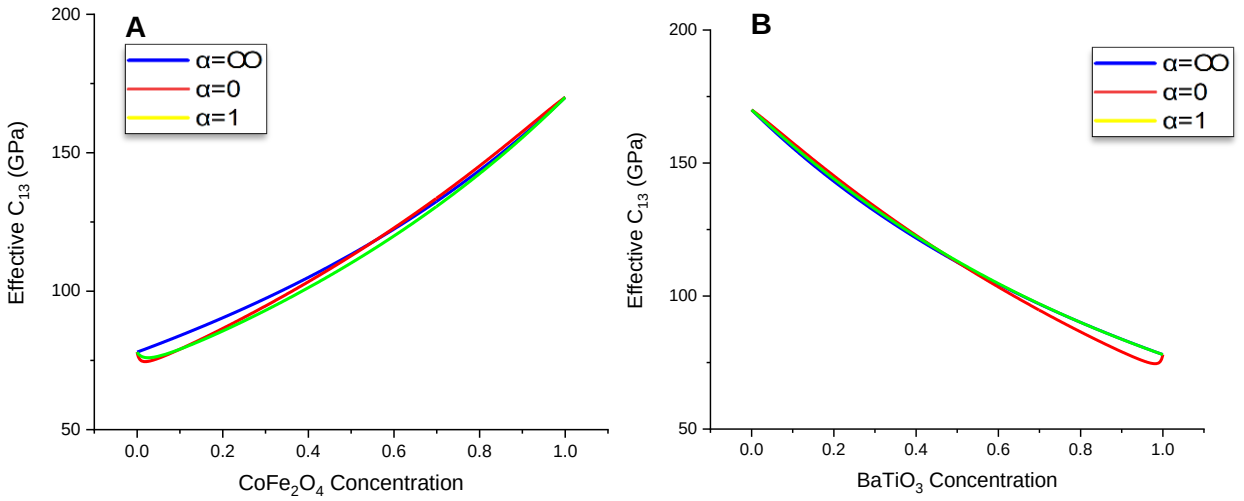

Fig 32. Elastic Constant C_{13} (a) CFO-in-BTO (b) BTO-in-CFO

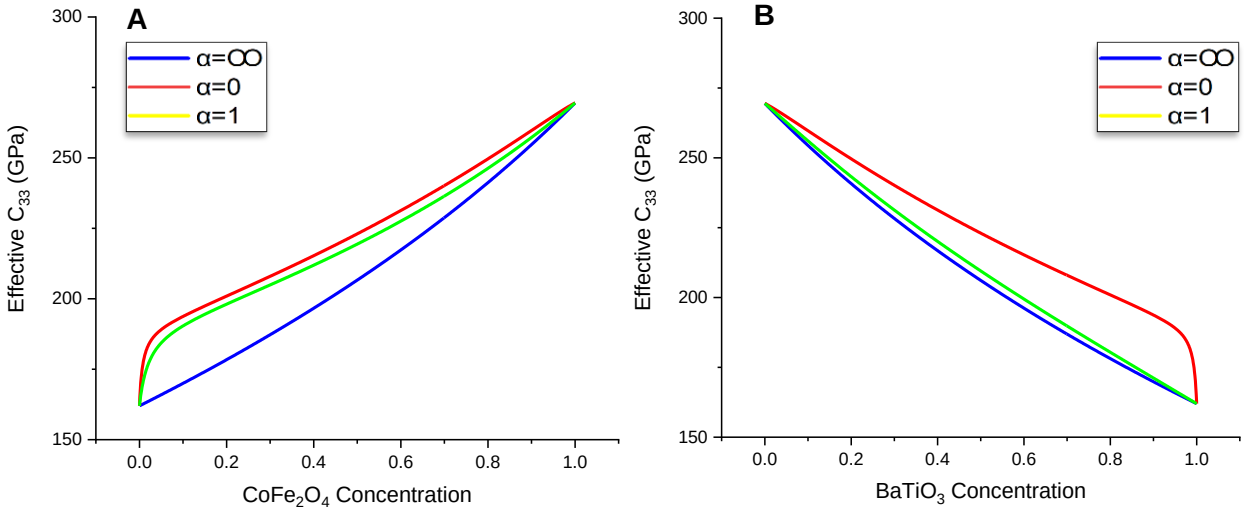

Fig 33. Elastic Constant C_{33} (a) CFO-in-BTO (b) BTO-in-CFO

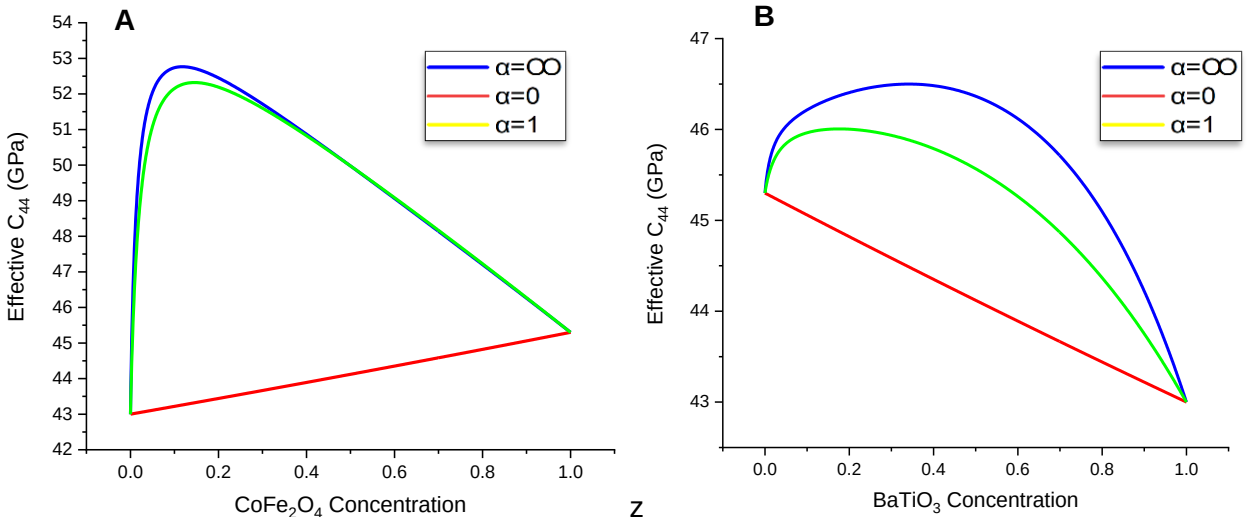

Fig 34. Elastic Constant C_{44} (a) CFO-in-BTO (b) BTO-in-CFO

5.2 Imperfect Interface

5.2.1 Magneto electric Coupling coefficients α_{11}, α_{33}

The magneto electric coefficient In the transverse direction, α_{11} and in axial direction, α_{33} are shown in Fig 35(a),(b) and in Fig 36(a),(b) for CFO-in-BTO and BTO-in-CFO, respectively for different inclusion concentration and aspect ratios. The overall shape of the curve for magneto electric coupling coefficient against inclusion concentration is similar for perfect interface and an imperfect interface which can be seen by comparing Fig. 18-19 and Fig. 35-36. From the figures it can be seen that the magneto electric coupling coefficient for an imperfect interface is lower compared to a perfect interface for all the aspect ratios.

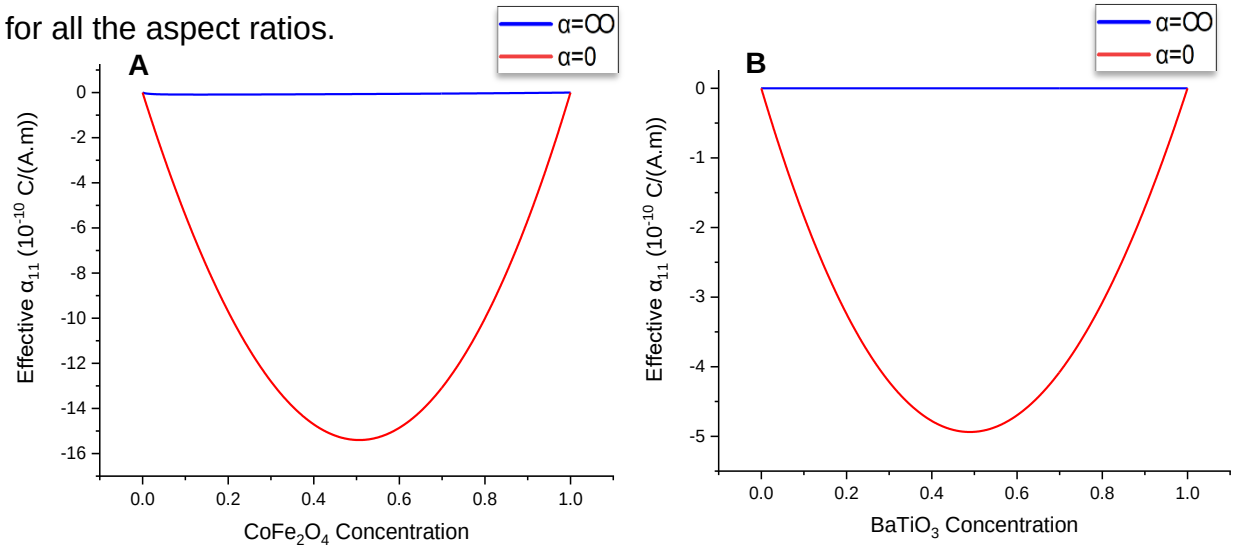

Fig 35. Magneto electric Coupling Coefficient α_{11} (a) CFO-in-BTO (b) BTO-in-CFO

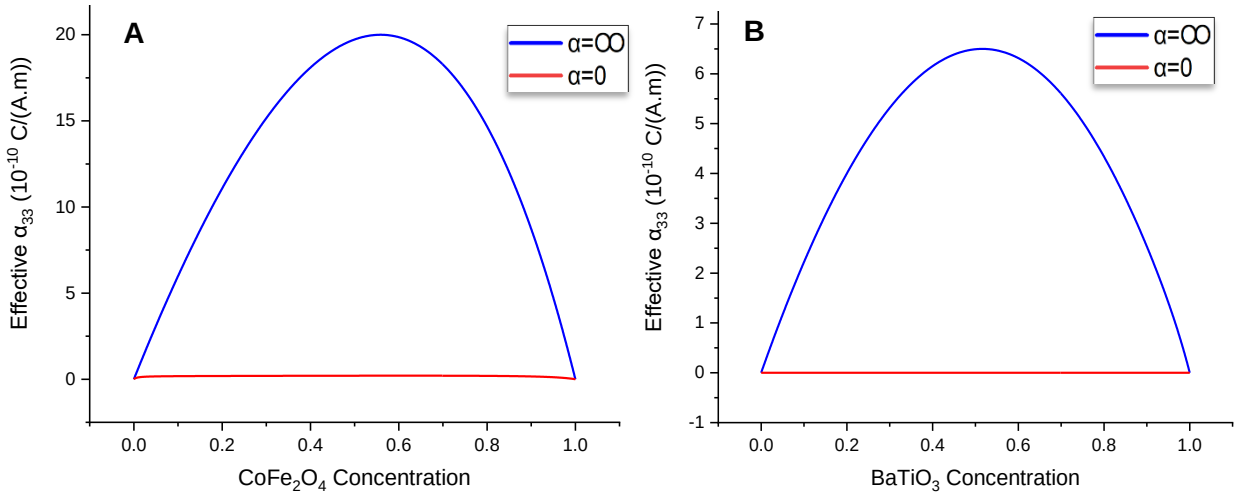

Fig 36. Magneto electric Coupling Coefficient α_{33} (a) CFO-in-BTO (b) BTO-in-CFO

5.2.2 Piezoelectric coefficients e_{15}, e_{31}, e_{33}

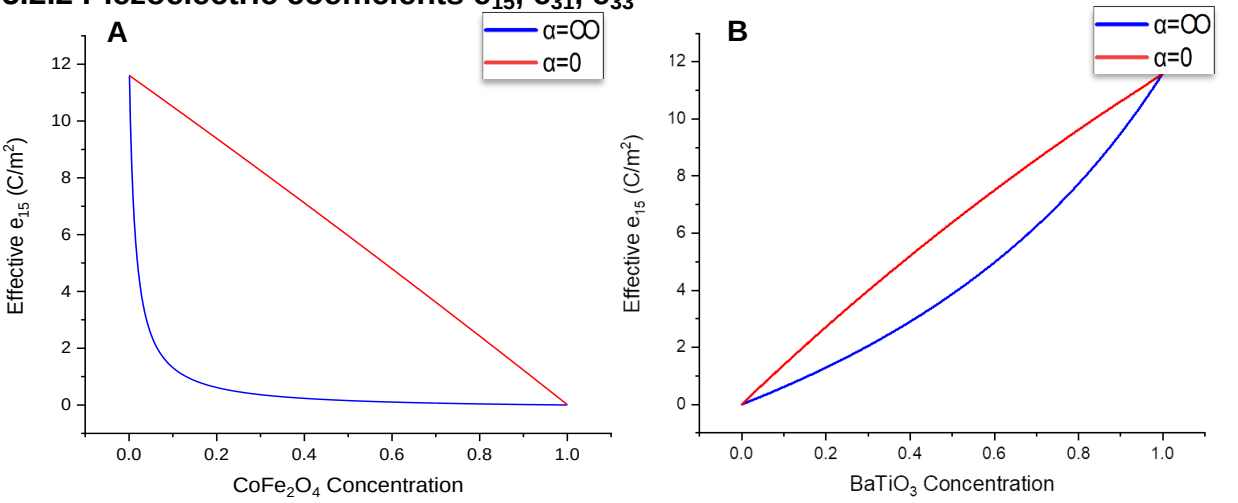

Fig 37. Piezoelectric Constant e_{15} (a) CFO-in-BTO (b) BTO-in-CFO

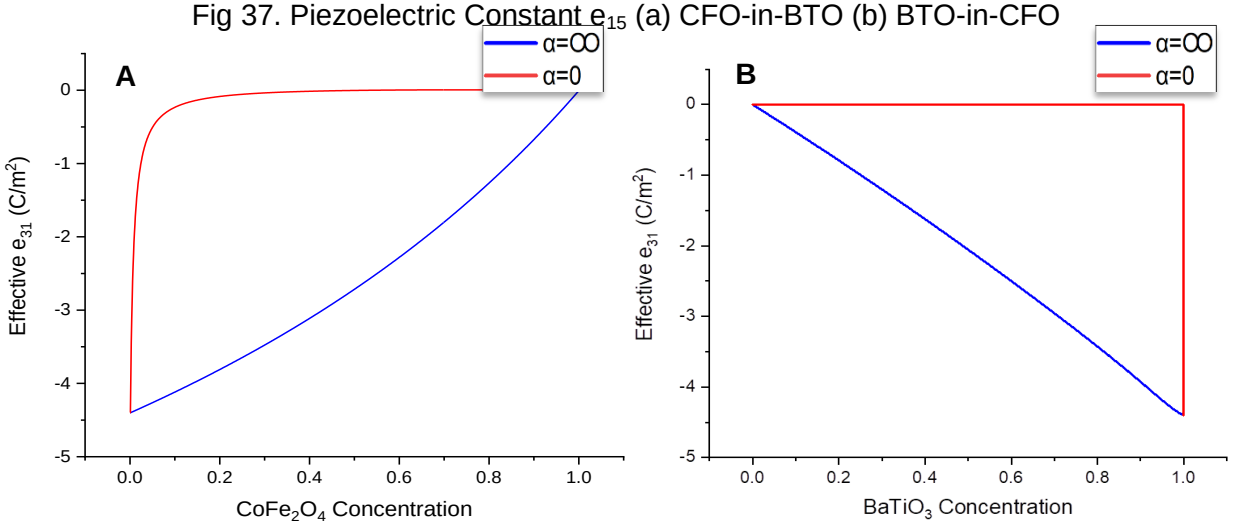

Fig 38. Piezoelectric Constant e_{31} (a) CFO-in-BTO (b) BTO-in-CFO

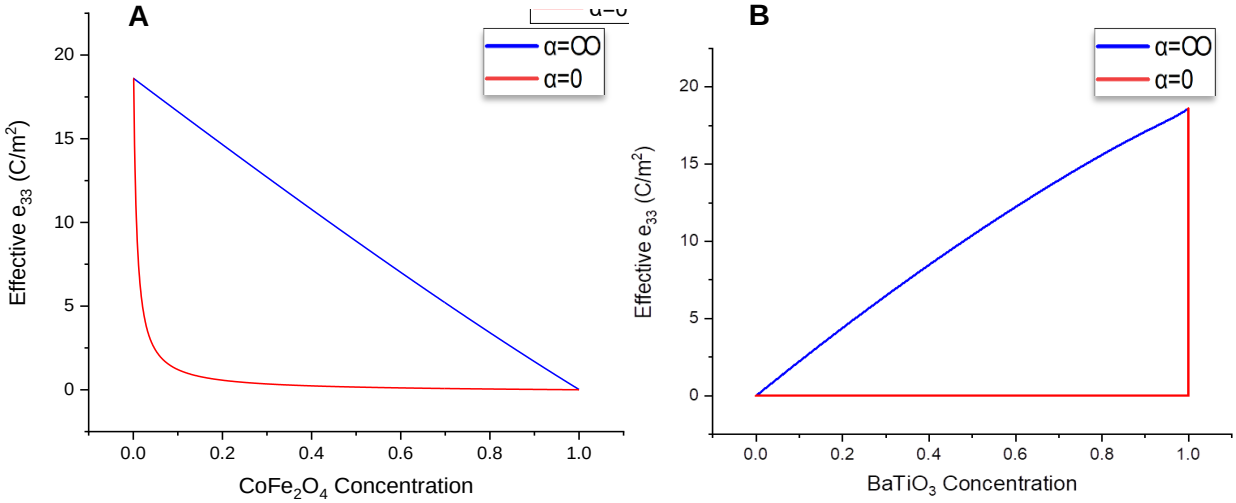

Fig 39. Piezoelectric Constant e_{33} (a) CFO-in-BTO (b) BTO-in-CFO

The piezoelectric constants e_{15}, e_{31}, e_{33} are plotted against different inclusion concentration and aspect ratios in Fig. 37-39 for CFO-in-BTO and BTO-in-CFO. Similar to the perfect interface plots for CFO-in-BTO and BTO-in-CFO, they both are mirror images of each other. The overall shape of the curve for perfect interface and an imperfect interface is similar which can be seen by comparing Fig. 20-22 and Fig. 37-39. From the plots it can be also seen that the piezoelectric coefficient for an imperfect interface is significantly lower compared to a perfect interface in e_{15}, and e_{31} but the reduction is not significant in e_{33} for all the aspect ratios.

5.2.3 Piezomagnetic coefficients q_{15}, q_{31}, q_{33}

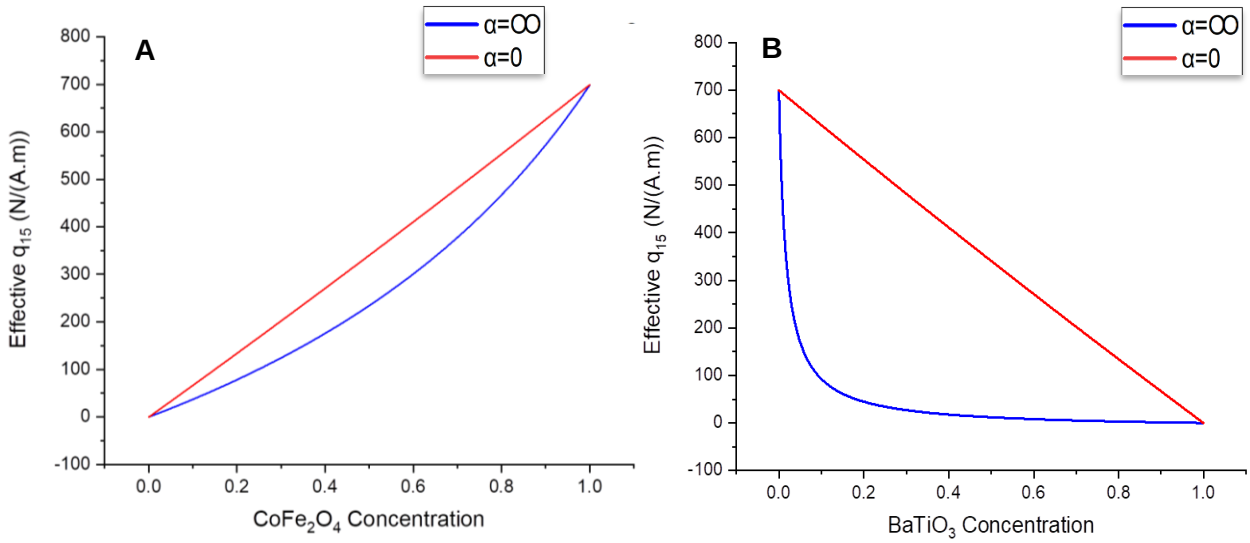

Fig 40. Piezo magnetic Constant q_{15} (a) CFO-in-BTO (b) BTO-in-CFO

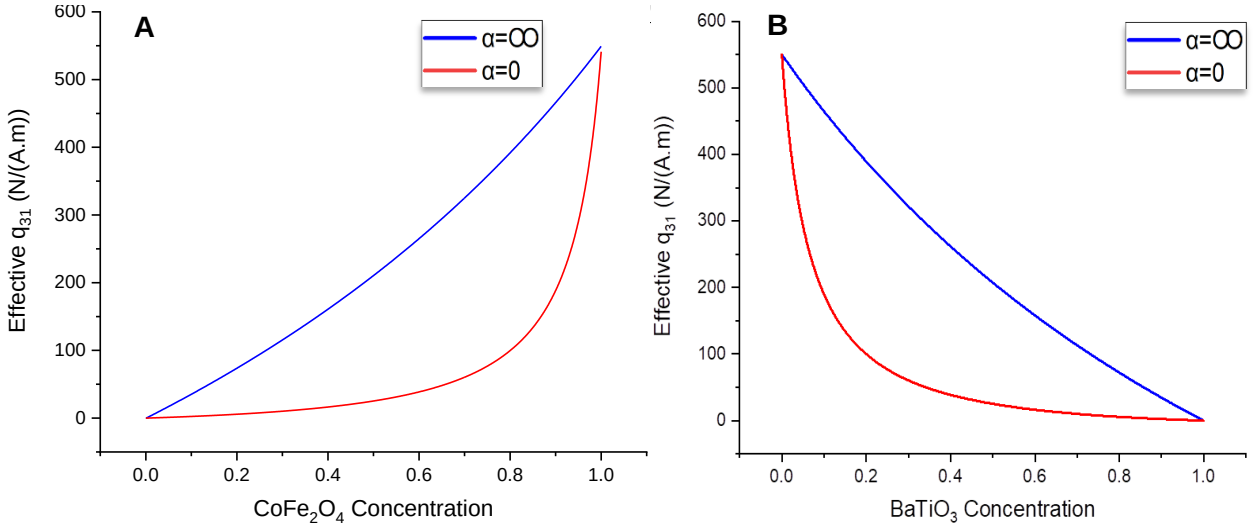

Fig 41. Piezo magnetic Constant q_{31} (a) CFO-in-BTO (b) BTO-in-CFO

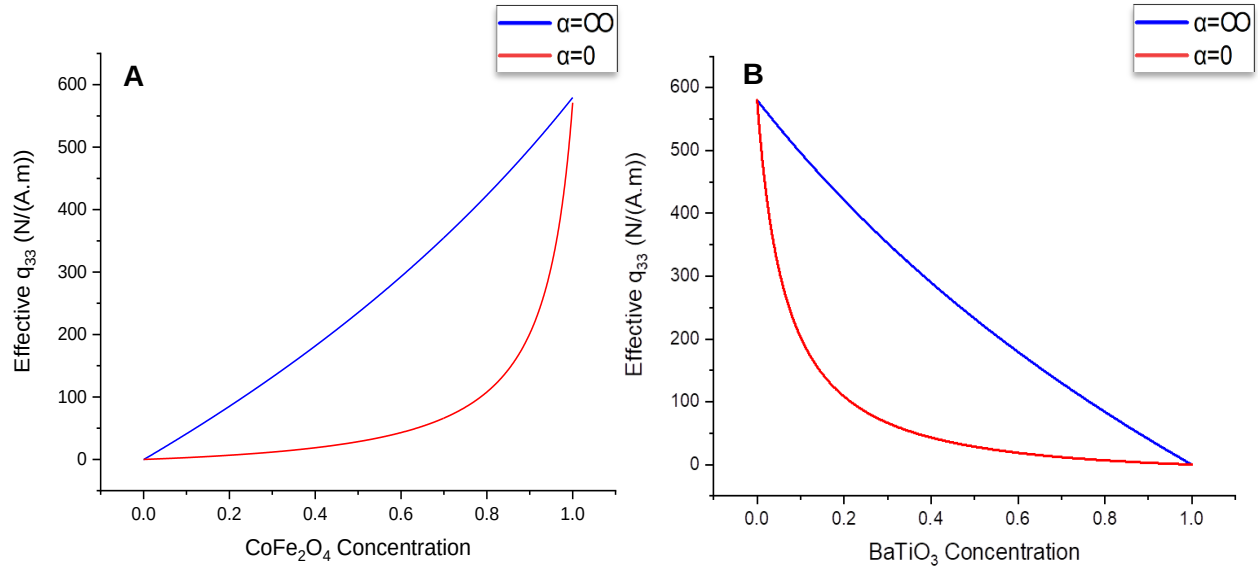

Fig 42. Piezo magnetic Constant q_{33} (a) CFO-in-BTO (b) BTO-in-CFO

The piezo magnetic constants q_{15}, q_{31}, q_{33} are plotted against different inclusion concentration and aspect ratios in Fig. 40-42 for CFO-in-BTO and BTO-in-CFO. The overall shape of the curve for piezo magnetic coefficient is similar for perfect interface and an imperfect interface which can be seen by comparing Fig. 23-25 and Fig. 40-42. From the plots it can also be seen that the piezo magnetic coefficient for an imperfect interface is not significantly lower compared to a perfect interface for all the aspect ratios.

5.2.4 Electric Permittivity κ_{11}, κ_{33}

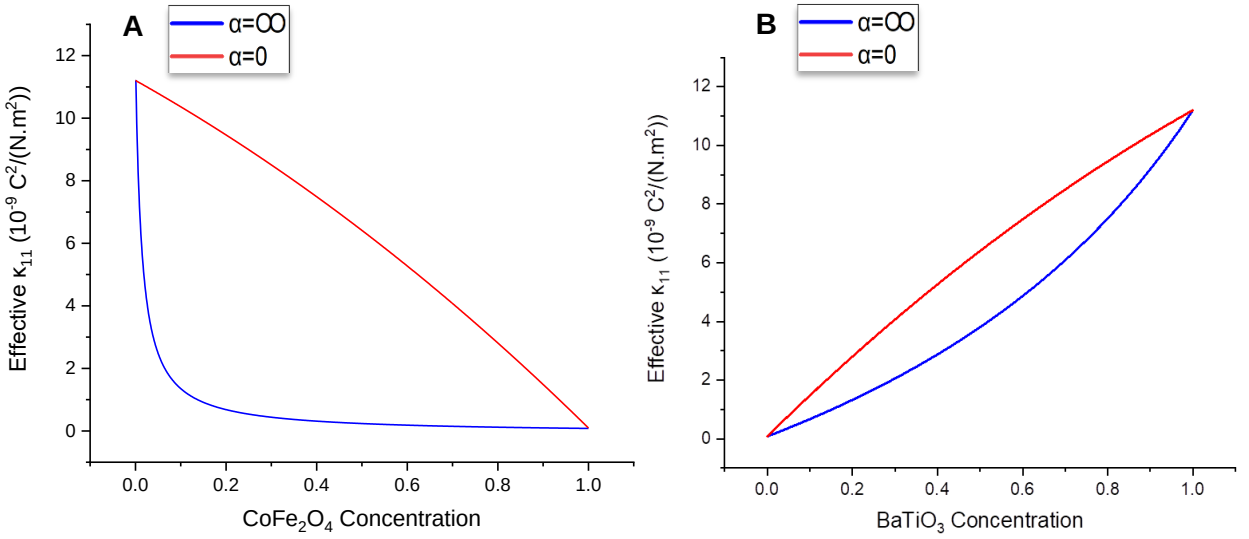

Fig 43. Electric Permittivity κ_{11} (a) CFO-in-BTO (b) BTO-in-CFO

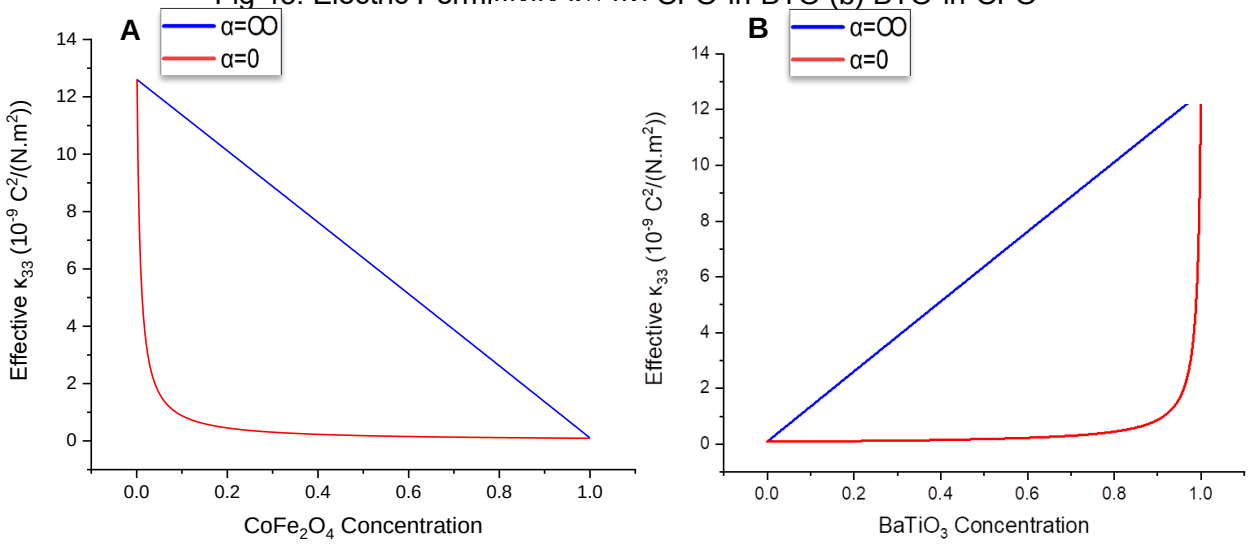

Fig 44. Electric Permittivity κ_{33} (a) CFO-in-BTO (b) BTO-in-CFO

The electric permittivity κ_{33}, κ_{11} are plotted against different inclusion concentration and aspect ratios in Fig. 43-44 for CFO-in-BTO and BTO-in-CFO. The overall shape of the curve for electric permittivity is similar for perfect interface and an imperfect interface which can be seen by comparing Fig. 26-27 and Fig. 43-44. From the plots it can be seen that the electric permittivity for an imperfect interface is significantly lower compared to a perfect interface for all the aspect ratios.

5.2.5 Magnetic Permeability μ_{11}, μ_{33}

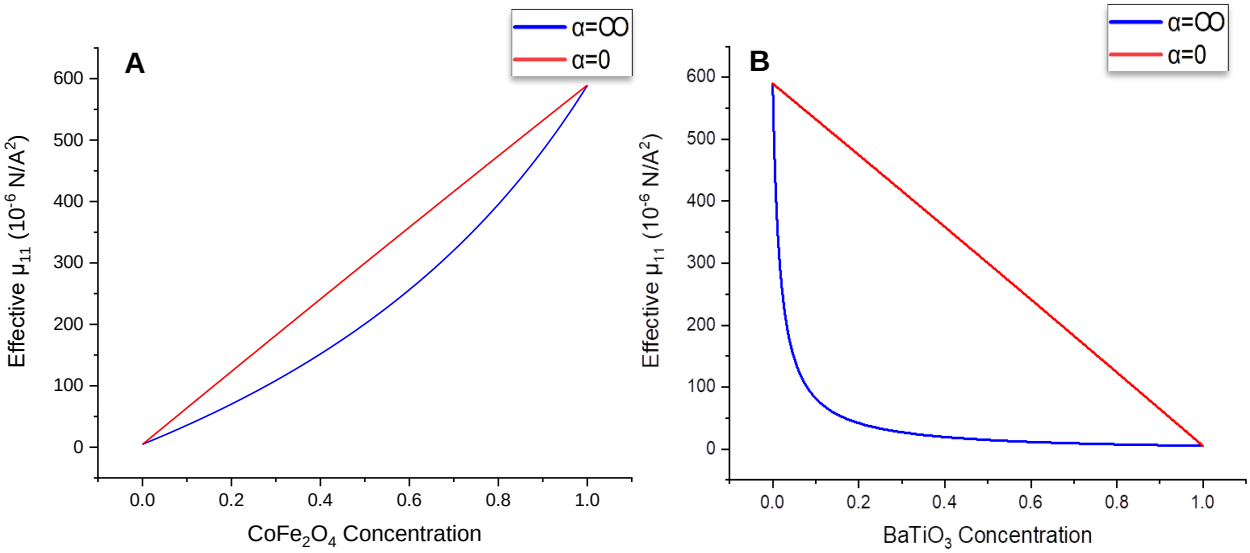

Fig 45. Magnetic Permeability μ_{11} (a) CFO-in-BTO (b) BTO-in-CFO

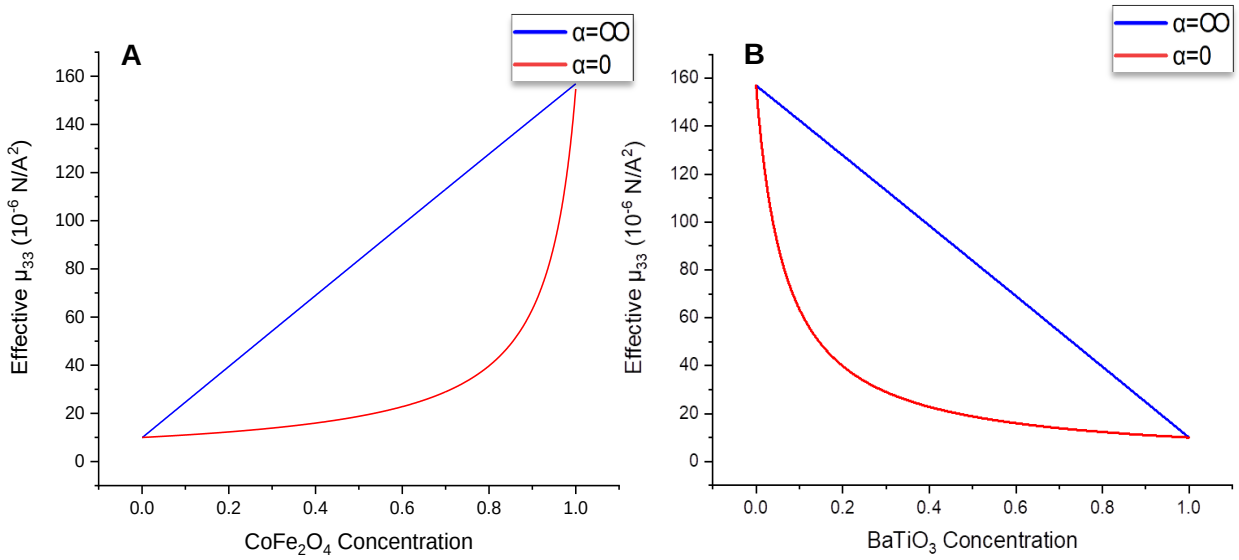

Fig 46. Magnetic Permeability μ_{33} (a) CFO-in-BTO (b) BTO-in-CFO

The magnetic permeability μ_{33}, μ_{11} are plotted against different inclusion concentration and aspect ratios in Fig. 45-46 for CFO-in-BTO and BTO-in-CFO. The overall shape of the curve for magnetic permeability is similar for perfect interface and an imperfect interface which can be seen by comparing Fig. 28-29 and Fig. 45-46. From the figures it can be seen that the magnetic permeability for an imperfect interface is not significantly reduced lower compared to a perfect interface for all the aspect ratios.

5.2.6 Elastic Constants C_{11}, C_{12}, C_{13}, C_{33}, C_{44}

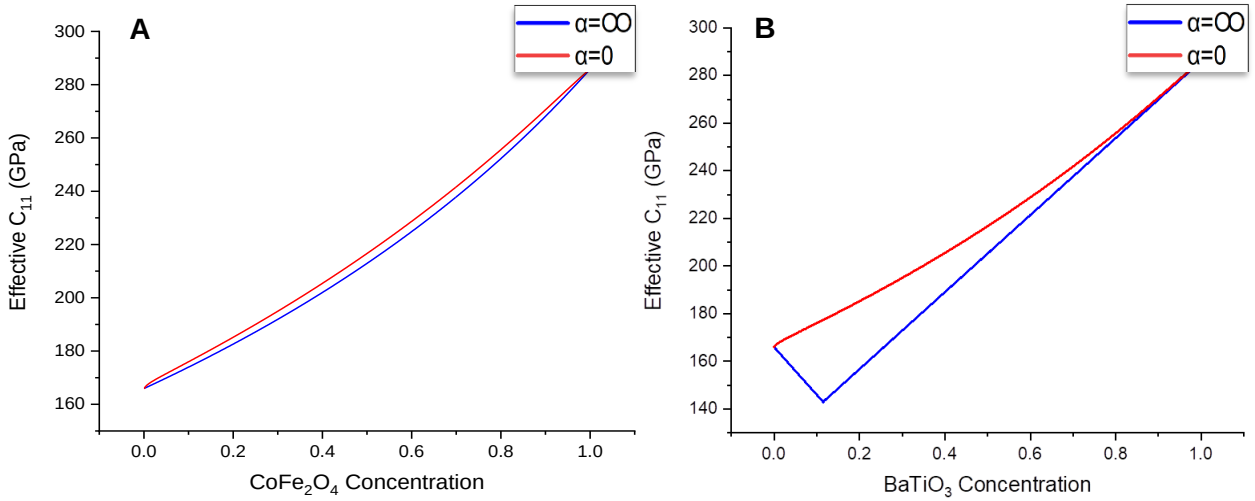

Fig 47. Elastic Constant C_{11} (a) CFO-in-BTO (b) BTO-in-CFO

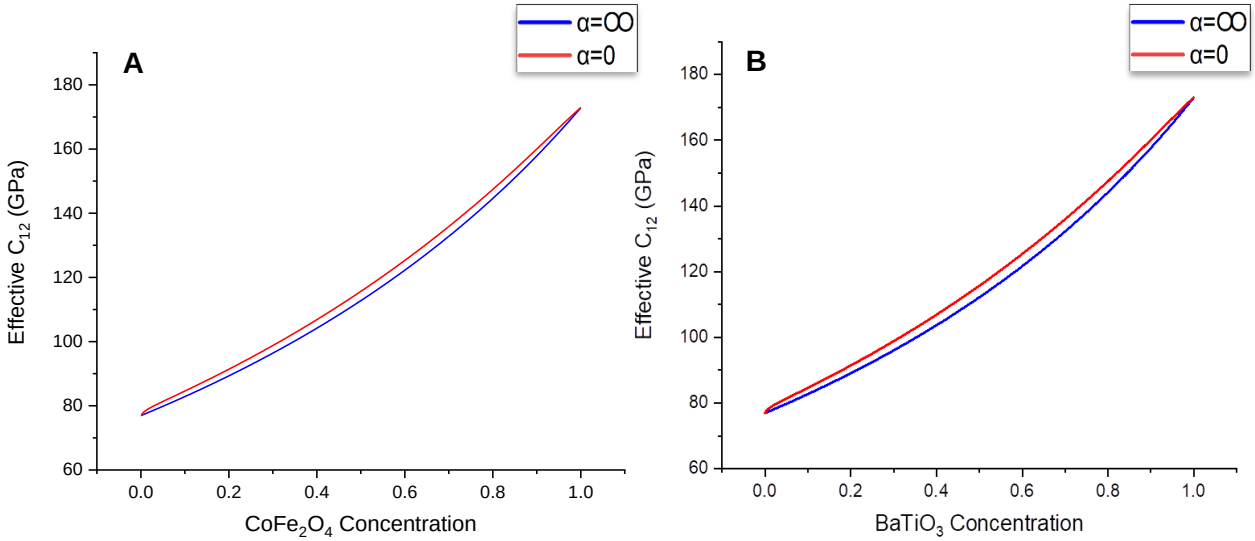

Fig 48. Elastic Constant C_{12} (a) CFO-in-BTO (b) BTO-in-CFO

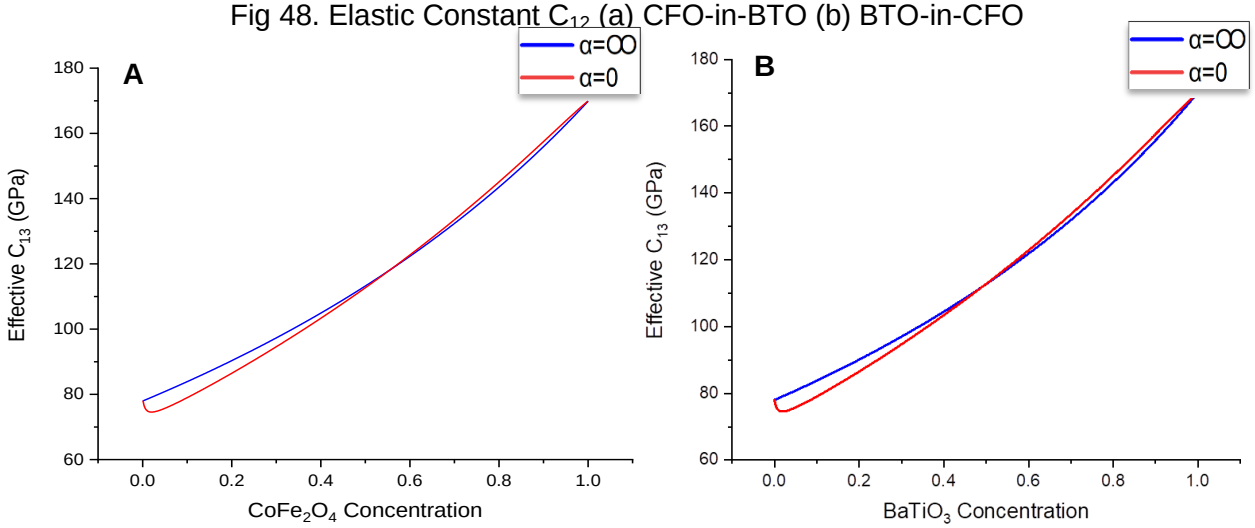

Fig 49. Elastic Constant C_{13} (a) CFO-in-BTO (b) BTO-in-CFO

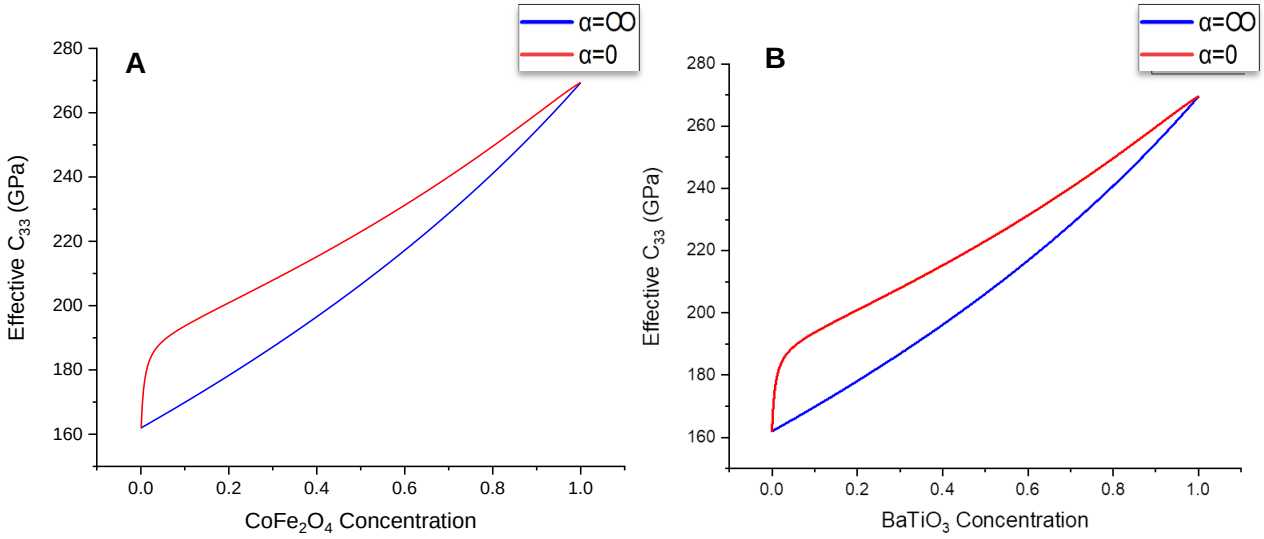

Fig 50. Elastic Constant C_{33} (a) CFO-in-BTO (b) BTO-in-CFO

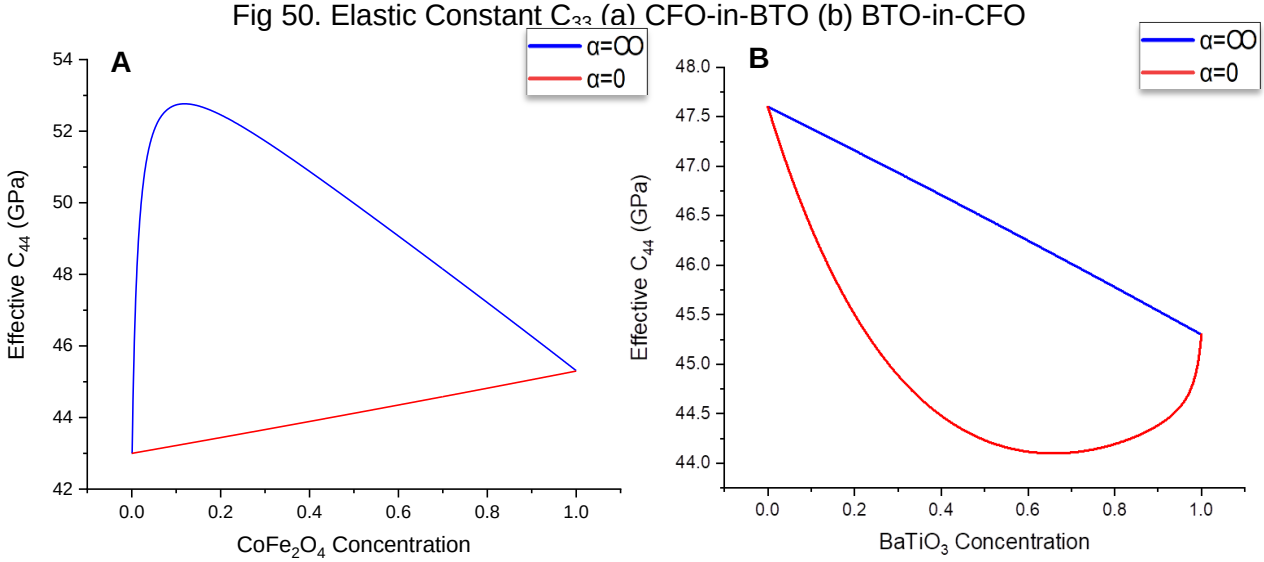

Fig 51. Elastic Constant C_{44} (a) CFO-in-BTO (b) BTO-in-CFO

The Elastic constants C_{11}, C_{12}, C_{13}, C_{33} and C_{44} are plotted against different inclusion concentration and aspect ratios in Fig. 47-51 for CFO-in-BTO and BTO-in-CFO. The values for imperfect interface are significantly lower compared to perfect interface which can be clearly seen by comparing Fig. 30-34 and Fig. 47-51. The elastic constant C_{11} in BTO-in-CFO for perfect interface was independent of the aspect ratio which is not the case for imperfect interface; fibrous composite has significantly lower value compared to multilayered composite. Other Elastic constants are equally reduced in BTO-in-CFO and CFO-in-BTO for an imperfect interface compared to a perfect interface.

Chapter 6 Future Work

We predicted the effective properties of multiferroic composites using micromechanical analysis for 3 aspect ratios of inclusion, $\alpha=0,1,\infty$ and distribution of the inclusion was considered uniform. In real life scenario the aspect ratio may not be constant throughout the composite and also the distribution of the inclusion may not be uniform. Owing to this fact, even when we have predicted the effective properties of multiferroic composites; we are unable to synthesize them because the uniform distribution and constant aspect ratio all throughout the composite is difficult to achieve with the existing technology.

To calculate effective properties of multiferroic composites having random distribution and random aspect ratio, we can use finite element analysis (FEA). But until now, not much research has been done in predicting effective properties of multiferroic composites using FEA. The problem that arises is that there is no code/software that can predict all the 3 properties; elastic, piezoelectric, piezomagentic at the same time. Finite Element Analysis requires 3 degrees of freedom to predict elastic properties, 4 degrees of freedom to predict piezoelectric/piezomagnetic properties and therefore it would require 5 degrees of freedom to predict multiferroic properties. There is no software as of now that can perform such kind of simulation. We would have to create a new software that can handle such simulations.

Chapter 7 References

[1] V. K. Wadhawan, “Towards a rigorous definition of ferroic phase transitions,” *Phase Transitions*, vol. 64, no. 3, pp. 165–177, 1998.

[2] R. Hill, “Theory of mechanical properties of fibre-strengthened materials: I. Elastic behaviour,” *J. Mech. Phys. Solids*, vol. 12, no. 4, pp. 199–212, Sep. 1964.

[3] M. Milgrom and S. Shtrikman, “Linear response of two-phase composites with cross moduli: Exact universal relations,” *Phys. Rev. A*, vol. 40, no. 3, pp. 1568–1575, Aug. 1989.

[4] J. van Suchtelen, “Product properties: A new Application of Composite Materials,” *Philips Res. Rep.*, vol. 27, pp. 28–37, 1972.

[5] C.-W. Nan, “Magnetoelectric effect in composites of piezoelectric and piezomagnetic phases,” *Phys. Rev. B*, vol. 50, no. 9, pp. 6082–6088, Sep. 1994.

[6] Y. Benveniste, “Magnetoelectric effect in fibrous composites with piezoelectric and piezomagnetic phases,” *Phys. Rev. B*, vol. 51, no. 22, pp. 16424–16427, Jun. 1995.

[7] E. J. Douglas and P. R. Ernst, “The determination of the elastic field of an ellipsoidal inclusion, and related problems,” *Proc. R. Soc. London. Ser. A. Math. Phys. Sci.*, vol. 241, no. 1226, pp. 376–396, Aug. 1957.

[8] W. Biao, “Three-dimensional analysis of an ellipsoidal inclusion in a piezoelectric material,” *Int. J. Solids Struct.*, vol. 29, no. 3, pp. 293–308, Jan. 1992.

[9] T. Chen, “Piezoelectric properties of multiphase fibrous composites: Some theoretical results,” *J. Mech. Phys. Solids*, vol. 41, no. 11, pp. 1781–1794, Nov. 1993.

[10] T. Chen, “Exact moduli and bounds of two-phase composites with coupled multifield linear responses,” *J. Mech. Phys. Solids*, vol. 45, no. 3, pp. 385–398, Mar. 1997.

[11] M. L. Dunn and M. Taya, “An Analysis of Piezoelectric Composite Materials Containing Ellipsoidal Inhomogeneities,” *Proc. Math. Phys. Sci.*, vol. 443, no. 1918, pp. 265–287, 1993.

[12] M. L. Dunn and H. A. Wienecke, “Green’s functions for transversely isotropic

piezoelectric solids," *Int. J. Solids Struct.*, vol. 33, no. 30, pp. 4571–4581, Dec. 1996.

[13] M. L. Dunn and M. Taya, "Micromechanics predictions of the effective electroelastic moduli of piezoelectric composites," *Int. J. Solids Struct.*, vol. 30, no. 2, pp. 161–175, Jan. 1993.

[14] J. H. Huang and J. S. Yu, "Electroelastic Eshelby tensors for an ellipsoidal piezoelectric inclusion," *Compos. Eng.*, vol. 4, no. 11, pp. 1169–1182, Jan. 1994.

[15] J. H. Huang and W.-S. Kuo, "The analysis of piezoelectric/piezomagnetic composite materials containing ellipsoidal inclusions," *J. Appl. Phys.*, vol. 81, no. 3, pp. 1378–1386, Feb. 1997.

[16] J. Y. Li and M. L. Dunn, "Anisotropic coupled-field inclusion and inhomogeneity problems," *Philos. Mag. A*, vol. 77, no. 5, pp. 1341–1350, May 1998.

[17] Y. Mikata, "Explicit determination of piezoelectric Eshelby tensors for a spheroidal inclusion," *Int. J. Solids Struct.*, vol. 38, no. 40–41, pp. 7045–7063, Oct. 2001.

[18] Y. Mikata, "Determination of piezoelectric Eshelby tensor in transversely isotropic piezoelectric solids," *Int. J. Eng. Sci.*, vol. 38, no. 6, pp. 605–641, Apr. 2000.

[19] S. Srinivas, J. Y. Li, Y. C. Zhou, and A. K. Soh, "The effective magnetoelectroelastic moduli of matrix-based multiferroic composites," *J. Appl. Phys.*, vol. 99, no. 4, p. 043905, Feb. 2006.

[20] X. Wang and E. Pan, "Magnetoelectric effects in multiferroic fibrous composite with imperfect interface," *Phys. Rev. B*, vol. 76, no. 21, p. 214107, Dec. 2007.

Chapter 8 Appendix

8.1 Eshelby's Tensor

8.1.1 Eshelby's Tensor for Aspect Ratio equal to infinity

Piezoelectric Matrix (BTO)

$$S_{11} = S_{22} = \frac{5C_{11} + C_{12}}{8C_{11}}$$

$$S_{12} = S_{21} = -\frac{1}{8} + \frac{3C_{12}}{8C_{11}}$$

$$S_{13} = S_{23} = \frac{C_{13}}{2C_{11}}$$

$$S_{19} = S_{29} = \frac{e_{31}}{2C_{11}}$$

$$S_{66} = \frac{3}{4} - \frac{C_{12}}{4C_{11}}$$

$$S_{44} = S_{55} = S_{77} = S_{88} = S_{10,10} = S_{11,11} = \frac{1}{2}$$

All other components zero.

Piezomagnetic Matrix (CFO)

$$S_{11} = S_{22} = \frac{5C_{11} + C_{12}}{8C_{11}}$$

$$S_{12} = S_{21} = -\frac{1}{8} + \frac{3C_{12}}{8C_{11}}$$

$$S_{13} = S_{23} = \frac{C_{13}}{2C_{11}}$$

$$S_{1,12} = S_{2,12} = \frac{q_{31}}{2C_{11}}$$

$$S_{66} = \frac{3}{4} - \frac{C_{12}}{4C_{11}}$$

$$S_{44} = S_{55} = S_{77} = S_{88} = S_{10,10} = S_{11,11} = \frac{1}{2}$$

All other components zero.

8.1.2 Eshelby's Tensor for Aspect Ratio equal zero

Piezoelectric Matrix (BTO)

$$S_{31} = S_{32} = \frac{e_{31}e_{33} + C_{13}\kappa_{33}}{e_{33}^{\ 2} + C_{33}\kappa_{33}}$$

$$S_{57} = S_{48} = \frac{e_{15}}{C_{44}}$$

$$S_{91} = S_{92} = \frac{-C_{33}e_{31} + C_{13}e_{33}}{e_{33}^{\ 2} + C_{33}\kappa_{33}}$$

$$S_{33} = S_{44} = S_{55} = S_{99} = S_{12,12} = 1$$

All other components zero.

Piezomagnetic Matrix (CFO)

$$S_{31} = S_{32} = \frac{q_{31}q_{33} + C_{13}\mu_{33}}{q_{33}^{\ 2} + C_{33}\mu_{33}}$$

$$S_{5,10} = S_{4,11} = \frac{q_{15}}{C_{44}}$$

$$S_{12,1} = S_{12,2} = \frac{-C_{33}q_{31} + C_{13}q_{33}}{q_{33}^{\ 2} + C_{33}\mu_{33}}$$

$$S_{33} = S_{44} = S_{55} = S_{99} = S_{12,12} = 1$$

All other components zero.

8.1.3 Eshelby's Tensor for Aspect Ratio other than zero and infinity

$$L_{ijMN}\begin{cases} C_{iJMn} & J,M=1,2,3 \\ e_{niJ} & J=1,2,3;M=4 \\ q_{niJ} & J=1,2,3;M=5 \\ e_{iMn} & J=4;M=1,2,3 \\ q_{iMn} & J=5;M=1,2,3 \\ -\kappa_{in} & J=4,M=4 \\ -\alpha_{in} & J=4,M=5;J=5,M=4 \\ -\mu_{in} & J=5,M=5 \end{cases}$$

With L_{iJMn} we introduce a 5x5 matrix K_{MJ}, $K_{MJ}=L_{iJMn}x_i x_n$, where $x_i=\left[x_1,x_2,x_3\right]^T$.

Then we define another pseudo tensor J_{inMJ}, $J_{inMJ}(x_1,x_2,x_3)=x_i x_n K^{-1}_{MJ}$, which is a function of x_1, x_2, x_3. Then we integrate J_{inMJ} over the volume of an ellipsoid inclusion Ω: $x_1^2/a_1^2+x_2^2/a_2^2+x_3^2/a_3^2\le 1$. When this inclusion is spheroidal and symettric about three-dimension, it satisfies $a_1=a_2$ and $\alpha=a_3/a_1$, where α is the aspect ratio of inclusions used. Hence the volume integral of J_{inMJ} can be written as

$$H_{inMJ}=\int_\Omega J_{inMJ}(x_1/a_1,x_2/a_2,x_3/a_3)dV=\int_\Omega J_{inMJ}(x_1,x_2,x_3/\alpha)dV=\int_{-1}^{1}d\tau\int_0^{2\prod}J_{inMJ}(y_1,y_2,y_3/\alpha)d\theta$$

where the second quantity is based on the fact that J_{inMJ} is a homogeneous function of order 0; thus multiplying all the variables by a_1 will not affect the integration. The third quantity is given by applying a change of variables from x_1, x_2, x_3 to

$$y_1=\sqrt{1-\tau^2}\cos\theta,\ y_2=\sqrt{1-\tau^2}\sin\theta,\ y_3=\tau$$

With $\tau\in[-1,1]$ and $\theta\in[0,2\prod]$. Finally S-tensor is determined by

$$S_{MnAb}=\begin{cases}\dfrac{L_{iJAb}(H_{inMj}+H_{iMnJ})}{8\prod} & M=1\sim 3\\ \dfrac{L_{iJAb}H_{in4j}}{4\prod} & M=4\\ \dfrac{L_{iJAb}H_{in5j}}{4\prod} & M=5\end{cases}$$

Still S_{MnAb} is a pseudo tensor. For the convenience of calculations we now convert it into a 12x12 matrix S by the Voigt-Nye contract notations

8.2 Code

```
%% Constant Values BTO
C11_BTO=166*(10^9)
C12_BTO=77*(10^9)
C13_BTO=78*(10^9)
C33_BTO=162*(10^9)
C44_BTO=43*(10^9)
C66_BTO=(C11_BTO-C12_BTO)/2
e31_BTO=-4.4
e33_BTO=18.6
e15_BTO=11.6
q31_BTO=0
q33_BTO=0
q15_BTO=0
k11_BTO=11.2*(10^-9)
k33_BTO=12.6*(10^-9)
u11_BTO=5*(10^-6)
u33_BTO=10*(10^-6)

%% Constant Values CFO
C11_CFO=286*(10^9)
```

```
C12_CFO=173*(10^9)
C13_CFO=170*(10^9)
C33_CFO=269.5*(10^9)
C44_CFO=45.3*(10^9)
C66_CFO=(C11_CFO-C12_CFO)/2
e31_CFO=0
e33_CFO=0
e15_CFO=0
q31_CFO=550
q33_CFO=580.3
q15_CFO=699.7
k11_CFO=0.08*(10^-9)
k33_CFO=0.093*(10^-9)
u11_CFO=590*(10^-6)
u33_CFO=157*(10^-6)
I=eye(12,12)
L_BTO_matrix_22=[C11_BTO C12_BTO C13_BTO  0 0 0 0 0 e31_BTO 0 0 q31_BTO;
C12_BTO C11_BTO C13_BTO  0 0 0 0 0 e31_BTO 0 0 q31_BTO; C13_BTO C13_BTO
C33_BTO  0 0 0 0 0 e33_BTO 0 0 q33_BTO; 0 0 0 C44_BTO 0 0 0 e15_BTO 0 0 q15_BTO 0; 0
0 0 0 C44_BTO 0 e15_BTO 0 0 q15_BTO 0 0;0 0 0 0 0 C66_BTO 0 0 0 0 0 0;0 0 0 0 e15_BTO
0 -1*k11_BTO 0 0 0 0 0;0 0 0 e15_BTO 0 0 0 -1*k11_BTO 0 0 0 0;e31_BTO e31_BTO
e33_BTO 0 0 0 0 0 -1*k33_BTO 0 0 0;0 0 0 0 q15_BTO 0 0 0 0 -1*u11_BTO 0 0;0 0 0 q15_BTO
0 0 0 0 0 0 -1*u11_BTO 0;q31_BTO q31_BTO q33_BTO 0 0 0 0 0 0 0 0 -1*u33_BTO]
L_CFO_matrix_22=[C11_CFO C12_CFO C13_CFO  0 0 0 0 0 e31_CFO 0 0 q31_CFO;
C12_CFO C11_CFO C13_CFO  0 0 0 0 0 e31_CFO 0 0 q31_CFO; C13_CFO C13_CFO
C33_CFO  0 0 0 0 0 e33_CFO 0 0 q33_CFO; 0 0 0 C44_CFO 0 0 0 e15_CFO 0 0 q15_CFO 0;
0 0 0 0 C44_CFO 0 e15_CFO 0 0 q15_CFO 0 0;0 0 0 0 0 C66_CFO 0 0 0 0 0 0;0 0 0 0
e15_CFO 0 -1*k11_CFO 0 0 0 0 0;0 0 0 e15_CFO 0 0 0 -1*k11_CFO 0 0 0 0;e31_CFO
e31_CFO e33_CFO 0 0 0 0 0 -1*k33_CFO 0 0 0;0 0 0 0 q15_CFO 0 0 0 0 -1*u11_CFO 0 0;0 0
0 q15_CFO 0 0 0 0 0 0 -1*u11_CFO 0;q31_CFO q31_CFO q33_CFO 0 0 0 0 0 0 0 0 -
1*u33_CFO]
L_BTO_matrix_13=[C11_BTO C12_BTO C13_BTO  0 0 0 0 0 e31_BTO 0 0 q31_BTO;
C12_BTO C11_BTO C13_BTO  0 0 0 0 0 e31_BTO 0 0 q31_BTO; C13_BTO C13_BTO
C33_BTO  0 0 0 0 0 e33_BTO 0 0 q33_BTO; 0 0 0 C44_BTO 0 0 0 e15_BTO 0 0 q15_BTO 0; 0
```

0 0 0 C44_BTO 0 e15_BTO 0 0 q15_BTO 0 0;0 0 0 0 0 C66_BTO 0 0 0 0 0 0;0 0 0 0 e15_BTO 0 -1*k11_BTO 0 0 0 0 0;0 0 0 e15_BTO 0 0 0 -1*k11_BTO 0 0 0 0;e31_BTO e31_BTO e33_BTO 0 0 0 0 0 -1*k33_BTO 0 0 0;0 0 0 0 q15_BTO 0 0 0 0 -1*u11_BTO 0 0;0 0 0 q15_BTO 0 0 0 0 0 0 -1*u11_BTO 0;q31_BTO q31_BTO q33_BTO 0 0 0 0 0 0 0 0 -1*u33_BTO]
L_CFO_matrix_13=[C11_CFO C12_CFO C13_CFO 0 0 0 0 0 e31_CFO 0 0 q31_CFO; C12_CFO C11_CFO C13_CFO 0 0 0 0 0 e31_CFO 0 0 q31_CFO; C13_CFO C13_CFO C33_CFO 0 0 0 0 0 e33_CFO 0 0 q33_CFO; 0 0 0 C44_CFO 0 0 0 e15_CFO 0 0 q15_CFO 0; 0 0 0 0 C44_CFO 0 e15_CFO 0 0 q15_CFO 0 0;0 0 0 0 0 C66_CFO 0 0 0 0 0 0;0 0 0 0 e15_CFO 0 -1*k11_CFO 0 0 0 0 0;0 0 0 e15_CFO 0 0 0 -1*k11_CFO 0 0 0 0;e31_CFO e31_CFO e33_CFO 0 0 0 0 0 -1*k33_CFO 0 0 0;0 0 0 0 q15_CFO 0 0 0 0 -1*u11_CFO 0 0;0 0 0 q15_CFO 0 0 0 0 0 0 -1*u11_CFO 0;q31_CFO q31_CFO q33_CFO 0 0 0 0 0 0 0 0 -1*u33_CFO]

Multilayered Composite with BTO (BaTiO3) as matrix

S31_BTO_22=(e31_BTO*e33_BTO + C13_BTO*k33_BTO)/(e33_BTO*e33_BTO + C33_BTO*k33_BTO)
S32_BTO_22=S31_BTO_22
S48_BTO_22=e15_BTO/C44_BTO
S57_BTO_22=S48_BTO_22
S91_BTO_22=(-1*C33_BTO*e31_BTO + C13_BTO*e33_BTO)/(e33_BTO*e33_BTO + C33_BTO*k33_BTO)
S92_BTO_22=S91_BTO_22
S12_12_BTO_22 = 1, S99_BTO_22 = S12_12_BTO_22, S55_BTO_22 = S99_BTO_22, S44_BTO_22 = S55_BTO_22, S33_BTO_22 = S44_BTO_22
S_BTO_matrix_piezoelectric_22=[0 0 0 0 0 0 0 0 0 0 0;0 0 0 0 0 0 0 0 0 0 0;S31_BTO_22 S32_BTO_22 S33_BTO_22 0 0 0 0 0 0 0 0;0 0 0 S44_BTO_22 0 0 0 S48_BTO_22 0 0 0 0;0 0 0 0 S55_BTO_22 0 S57_BTO_22 0 0 0 0;0 0 0 0 0 0 0 0 0 0 0;0 0 0 0 0 0 0 0 0 0 0;0 0 0 0 0 0 0 0 0 0 0;S91_BTO_22 S92_BTO_22 0 0 0 0 0 0 S99_BTO_22 0 0 0;0 0 0 0 0 0 0 0 0 0 0;0 0 0 0 0 0 0 0 0 0 0;0 0 0 0 0 0 0 0 0 0 0;0 0 0 0 0 0 0 0 0 0 S12_12_BTO_22]
for i=0:1:1000
L_eff_BTO_matrix_22=L_BTO_matrix_22 + (1-(i/1000))*(L_CFO_matrix_22-L_BTO_matrix_22)*inv(I +

(i/1000)*S_BTO_matrix_piezoelectric_22*inv(L_BTO_matrix_22)*(L_CFO_matrix_22-L_BTO_matrix_22))

C11_eff_BTO_matrix_22(i+1)=L_eff_BTO_matrix_22(1,1)

C12_eff_BTO_matrix_22(i+1)=L_eff_BTO_matrix_22(1,2)

C13_eff_BTO_matrix_22(i+1)=L_eff_BTO_matrix_22(1,3)

C33_eff_BTO_matrix_22(i+1)=L_eff_BTO_matrix_22(3,3)

C44_eff_BTO_matrix_22(i+1)=L_eff_BTO_matrix_22(4,4)

e31_eff_BTO_matrix_22(i+1)=L_eff_BTO_matrix_22(9,1)

e33_eff_BTO_matrix_22(i+1)=L_eff_BTO_matrix_22(9,3)

e15_eff_BTO_matrix_22(i+1)=L_eff_BTO_matrix_22(8,4)

u11_eff_BTO_matrix_22(i+1)=L_eff_BTO_matrix_22(10,10)

u33_eff_BTO_matrix_22(i+1)=L_eff_BTO_matrix_22(12,12)

q31_eff_BTO_matrix_22(i+1)=L_eff_BTO_matrix_22(1,12)

q33_eff_BTO_matrix_22(i+1)=L_eff_BTO_matrix_22(3,12)

q15_eff_BTO_matrix_22(i+1)=L_eff_BTO_matrix_22(4,11)

k33_eff_BTO_matrix_22(i+1)=L_eff_BTO_matrix_22(9,9)

k11_eff_BTO_matrix_22(i+1)=L_eff_BTO_matrix_22(8,8)

alpha33_eff_BTO_matrix_22(1+i)=L_eff_BTO_matrix_22(12,9)

alpha11_eff_BTO_matrix_22(1+i)=L_eff_BTO_matrix_22(10,7)

end

Fibrous Composite with BTO (BaTiO3) as matrix

S11_BTO_13=(5*C11_BTO + C12_BTO)/(8*C11_BTO)

S22_BTO_13=S11_BTO_13

S12_BTO_13=(3*C12_BTO)/(8*C11_BTO)-1/8

S21_BTO_13=S12_BTO_13

S13_BTO_13=C13_BTO/(2*C11_BTO)

S23_BTO_13=S13_BTO_13

S19_BTO_13=e31_BTO/(2*C11_BTO)

S29_BTO_13=S19_BTO_13

S66_BTO_13=-1*(C12_BTO/(4*C11_BTO))+3/4

S11_11_BTO_13 = 1/2, S10_10_BTO_13 = S11_11_BTO_13, S77_BTO_13 = S10_10_BTO_13, S55_BTO_13 = S77_BTO_13, S44_BTO_13 = S55_BTO_13, S88_BTO_13 = S55_BTO_13

```
S_BTO_matrix_piezoelectric_13=[S11_BTO_13 S12_BTO_13 S13_BTO_13 0 0 0 0 0
S19_BTO_13 0 0 0;S21_BTO_13 S22_BTO_13 S23_BTO_13 0 0 0 0 0 S29_BTO_13 0 0 0;0 0
0 0 0 0 0 0 0 0 0 0;0 0 0 S44_BTO_13 0 0 0 0 0 0 0;0 0 0 0 S55_BTO_13 0 0 0 0 0 0 0;0 0 0 0
0 S66_BTO_13 0 0 0 0 0 0;0 0 0 0 0 0 S77_BTO_13 0 0 0 0 0;0 0 0 0 0 0 0 S88_BTO_13 0 0 0
0;0 0 0 0 0 0 0 0 0 0 0 0;0 0 0 0 0 0 0 0 0 S10_10_BTO_13 0 0;0 0 0 0 0 0 0 0 0 0
S11_11_BTO_13 0;0 0 0 0 0 0 0 0 0 0 0 0]
for i=0:1:1000
L_eff_BTO_matrix_13=L_BTO_matrix_13 + (1-(i/1000))*(L_CFO_matrix_13-
L_BTO_matrix_13)*inv(I +
(i/1000)*S_BTO_matrix_piezoelectric_13*inv(L_BTO_matrix_13)*(L_CFO_matrix_13-
L_BTO_matrix_13) )
C11_eff_BTO_matrix_13(1+i)=L_eff_BTO_matrix_13(1,1)
C12_eff_BTO_matrix_13(1+i)=L_eff_BTO_matrix_13(1,2)
C13_eff_BTO_matrix_13(1+i)=L_eff_BTO_matrix_13(1,3)
C33_eff_BTO_matrix_13(1+i)=L_eff_BTO_matrix_13(3,3)
C44_eff_BTO_matrix_13(1+i)=L_eff_BTO_matrix_13(4,4)
e31_eff_BTO_matrix_13(1+i)=L_eff_BTO_matrix_13(9,1)
e33_eff_BTO_matrix_13(1+i)=L_eff_BTO_matrix_13(9,3)
e15_eff_BTO_matrix_13(1+i)=L_eff_BTO_matrix_13(8,4)
u11_eff_BTO_matrix_13(1+i)=L_eff_BTO_matrix_13(10,10)
u33_eff_BTO_matrix_13(1+i)=L_eff_BTO_matrix_13(12,12)
q31_eff_BTO_matrix_13(1+i)=L_eff_BTO_matrix_13(1,12)
q33_eff_BTO_matrix_13(1+i)=L_eff_BTO_matrix_13(3,12)
q15_eff_BTO_matrix_13(1+i)=L_eff_BTO_matrix_13(4,11)
k33_eff_BTO_matrix_13(1+i)=L_eff_BTO_matrix_13(9,9)
k11_eff_BTO_matrix_13(1+i)=L_eff_BTO_matrix_13(8,8)
alpha33_eff_BTO_matrix_13(1+i)=L_eff_BTO_matrix_13(12,9)
alpha11_eff_BTO_matrix_13(1+i)=L_eff_BTO_matrix_13(10,7)
end
```

Multilayered Composite with CFO ($CoFe_2O_4$) as matrix

```
S31_CFO_22=(q31_CFO*q33_CFO + C13_CFO*u33_CFO)/(q33_CFO*q33_CFO +
C33_CFO*u33_CFO)
```

```
S32_CFO_22=S31_CFO_22
S5_10_CFO_22=q15_CFO/C44_CFO
S4_11_CFO_22=S5_10_CFO_22
S12_1_CFO_22=(-1*C33_CFO*q31_CFO + C13_CFO*q33_CFO)/(q33_CFO*q33_CFO +
C33_CFO*u33_CFO)
S12_2_CFO_22=S12_1_CFO_22
S12_12_CFO_22 = 1, S99_CFO_22 = S12_12_CFO_22, S55_CFO_22 = S99_CFO_22,
S44_CFO_22 = S55_CFO_22, S33_CFO_22 = S44_CFO_22
S_CFO_matrix_piezomagnetic_22=[0 0 0 0 0 0 0 0 0 0 0;0 0 0 0 0 0 0 0 0 0 0;S31_CFO_22
S32_CFO_22 S33_CFO_22 0 0 0 0 0 0 0 0;0 0 0 S44_CFO_22 0 0 0 0 0 S4_11_CFO_22
0;0 0 0 0 S55_CFO_22 0 0 0 0 S5_10_CFO_22 0 0;0 0 0 0 0 0 0 0 0 0 0;0 0 0 0 0 0 0 0 0 0
0;0 0 0 0 0 0 0 0 0 0 0;0 0 0 0 0 0 0 0 S99_CFO_22 0 0 0;0 0 0 0 0 0 0 0 0 0 0;0 0 0 0 0 0 0
0 0 0 0 0;S12_1_CFO_22 S12_2_CFO_22 0 0 0 0 0 0 0 0 S12_12_CFO_22]
for i=0:1:1000
L_eff_CFO_matrix_22=L_CFO_matrix_22 + (1-(i/1000))*(L_BTO_matrix_22-
L_CFO_matrix_22)*inv(I +
(i/1000)*S_CFO_matrix_piezomagnetic_22*inv(L_CFO_matrix_22)*(L_BTO_matrix_22-
L_CFO_matrix_22) )
C11_eff_CFO_matrix_22(i+1)=L_eff_CFO_matrix_22(1,1)
C12_eff_CFO_matrix_22(i+1)=L_eff_CFO_matrix_22(1,2)
C13_eff_CFO_matrix_22(i+1)=L_eff_CFO_matrix_22(1,3)
C33_eff_CFO_matrix_22(i+1)=L_eff_CFO_matrix_22(3,3)
C44_eff_CFO_matrix_22(i+1)=L_eff_CFO_matrix_22(4,4)
e31_eff_CFO_matrix_22(i+1)=L_eff_CFO_matrix_22(9,1)
e33_eff_CFO_matrix_22(i+1)=L_eff_CFO_matrix_22(9,3)
e15_eff_CFO_matrix_22(i+1)=L_eff_CFO_matrix_22(8,4)
u11_eff_CFO_matrix_22(i+1)=L_eff_CFO_matrix_22(10,10)
u33_eff_CFO_matrix_22(i+1)=L_eff_CFO_matrix_22(12,12)
q31_eff_CFO_matrix_22(i+1)=L_eff_CFO_matrix_22(1,12)
q33_eff_CFO_matrix_22(i+1)=L_eff_CFO_matrix_22(3,12)
q15_eff_CFO_matrix_22(i+1)=L_eff_CFO_matrix_22(4,11)
k33_eff_CFO_matrix_22(i+1)=L_eff_CFO_matrix_22(9,9)
k11_eff_CFO_matrix_22(i+1)=L_eff_CFO_matrix_22(8,8)
alpha33_eff_CFO_matrix_22(1+i)=L_eff_CFO_matrix_22(12,9)
```

alpha11_eff_CFO_matrix_22(1+i)=L_eff_CFO_matrix_22(10,7)
end

Fibrous Composite with CFO (CoFe2O4) as matrix

S11_CFO_13=(5*C11_CFO + C12_CFO)/(8*C11_CFO)
S22_CFO_13=S11_CFO_13
S12_CFO_13=(3*C12_CFO)/(8*C11_CFO)-1/8
S21_CFO_13=S12_CFO_13
S13_CFO_13=C13_CFO/(2*C11_CFO)
S23_CFO_13=S13_CFO_13
S1_12_CFO_13=q31_CFO/(2*C11_CFO)
S2_12_CFO_13=S1_12_CFO_13
S66_CFO_13=-1*(C12_CFO/(4*C11_CFO))+3/4
S11_11_CFO_13 = 1/2, S10_10_CFO_13 = S11_11_CFO_13, S77_CFO_13 = S10_10_CFO_13, S55_CFO_13 = S77_CFO_13, S44_CFO_13 = S55_CFO_13, S88_CFO_13 = S55_CFO_13
S_CFO_matrix_piezomagnetic_13=[S11_CFO_13 S12_CFO_13 S13_CFO_13 0 0 0 0 0 0 0 0 S1_12_CFO_13;S21_CFO_13 S22_CFO_13 S23_CFO_13 0 0 0 0 0 0 0 0 S2_12_CFO_13;0 0 0 0 0 0 0 0 0 0 0 0;0 0 0 S44_CFO_13 0 0 0 0 0 0 0 0;0 0 0 0 S55_CFO_13 0 0 0 0 0 0 0;0 0 0 0 0 S66_CFO_13 0 0 0 0 0 0;0 0 0 0 0 0 S77_CFO_13 0 0 0 0 0;0 0 0 0 0 0 0 S88_CFO_13 0 0 0 0;0 0 0 0 0 0 0 0 0 0 0 0;0 0 0 0 0 0 0 0 0 S10_10_CFO_13 0 0;0 0 0 0 0 0 0 0 0 0 S11_11_CFO_13 0;0 0 0 0 0 0 0 0 0 0 0 0]
for i=0:1:1000
L_eff_CFO_matrix_13=L_CFO_matrix_13 + (1-(i/1000))*(L_BTO_matrix_13-L_CFO_matrix_13)*inv(I + (i/1000)*S_CFO_matrix_piezomagnetic_13*inv(L_CFO_matrix_13)*(L_BTO_matrix_13-L_CFO_matrix_13))
C11_eff_CFO_matrix_13(1+i)=L_eff_CFO_matrix_13(1,1)
C12_eff_CFO_matrix_13(1+i)=L_eff_CFO_matrix_13(1,2)
C13_eff_CFO_matrix_13(1+i)=L_eff_CFO_matrix_13(1,3)
C33_eff_CFO_matrix_13(1+i)=L_eff_CFO_matrix_13(3,3)
C44_eff_CFO_matrix_13(1+i)=L_eff_CFO_matrix_13(4,4)
e31_eff_CFO_matrix_13(1+i)=L_eff_CFO_matrix_13(9,1)

```
e33_eff_CFO_matrix_13(1+i)=L_eff_CFO_matrix_13(9,3)
e15_eff_CFO_matrix_13(1+i)=L_eff_CFO_matrix_13(8,4)
u11_eff_CFO_matrix_13(1+i)=L_eff_CFO_matrix_13(10,10)
u33_eff_CFO_matrix_13(1+i)=L_eff_CFO_matrix_13(12,12)
q31_eff_CFO_matrix_13(1+i)=L_eff_CFO_matrix_13(1,12)
q33_eff_CFO_matrix_13(1+i)=L_eff_CFO_matrix_13(3,12)
q15_eff_CFO_matrix_13(1+i)=L_eff_CFO_matrix_13(4,11)
k33_eff_CFO_matrix_13(1+i)=L_eff_CFO_matrix_13(9,9)
k11_eff_CFO_matrix_13(1+i)=L_eff_CFO_matrix_13(8,8)
alpha33_eff_CFO_matrix_13(1+i)=L_eff_BTO_matrix_13(12,9)
alpha11_eff_CFO_matrix_13(1+i)=L_eff_BTO_matrix_13(10,7)
end
```